Bluck, B. J. 1964: Sedimentation of an alluvial fan in southern Nevada. *J. Sediment. Petrol.* 34, 395–400.

Bluck, B. J. 1979: Structure of coarse grained braided stream alluvium. *Trans. R. Soc. Edinb.*, 70, 181–221.

Bluck, B. J. 1982: Texture of gravel bars in Braided Streams. In R. D. Hey, J. C. Bathurst and C. R. Thorne (eds), *Gravel-bed Rivers*, Chichester: Wiley, 339–55.

Boothroyd, J. C. and Ashley, G. M. 1975: Process, bar morphology and sedimentary structures on braided outwash fans, northwestern Gulf of Alaska. In A. V. Jopling and B. McDonald (eds), *Glaciofluvial and Glaciolacustrine Sedimentation*, SEPM Spec. Publ. 23, 193–222.

Bowmann, D. 1977: Stepped bed morphology in arid gravelly channels. *Bull. Geol. Soc. America*, 88, 291–8.

Church, M. 1972: Baffin Island sandurs: a study of Arctic fluvial processes. *Geol. Surv. Canada Bull.*, 216.

Church, M. and Jones, D. 1982: Channel bars in gravel bed rivers. In R. D. Hey, J. C. Bathurst and C. R. Thorne (eds), *Gravel-bed Rivers*, Chichester: Wiley, 291–324.

Church, M. and Kellerhals, R. 1978: On statistics of grain size variation along a gravel river. *Can. J. Earth Sci.*, 15, 1151–60.

Cooke, R. U. and Warren, A. 1973: *Geomorphology in Deserts*. London: Batsford.

Eckis, R. 1928: Alluvial fans in the Cucamonga District, southern California. *J. Geol.*, 36, 224–7.

Ferguson, R. I. and Werritty, A. 1983: Bar development and channel changes in the gravelly River Feshie, Scotland. In J. D. Collinson and J. Lewin (eds), *Modern and Ancient Fluvial Systems*, Int. Assoc. Sedimentologists, Spec. Publ. 6, 181–93.

Hooke, R. Le B. 1968: Steady-state relationships on arid-region alluvial fans in closed basins. *Am. J. Sci.*, 266, 609–29.

Knighton, A. D. 1980: Longitudinal changes in size and sorting of stream-bed material in four English rivers. *Bull. Geol. Soc. America*, 91, 55–62.

Krumbein, W. C. 1940: Flood gravels of San Gabriel Canyon, California. *Bull. Geol. Soc. America*, 51, 639–76.

Krumbein, W. C. 1942: Flood deposits of Arroyo Seco, Los Angeles County, California. *Bull. Geol. Soc. America*, 53, 1355–402.

Lewin, J. 1981: Contemporary erosion and sedimentation. In J. Lewin (ed.), *British Rivers*, London: Allen and Unwin, 34–58.

McDonald, B. C. and Banerjee, I. 1971: Sediments and bedforms on a braided outwash plain. *Can. J. Earth Sci.*, 8, 1282–301.

Pettijohn, F. J. 1975: *Sedimentary Rocks*. London: Harper Row.

Rust, B. R. 1972: Structure and process in a braided river. *Sedimentology*, 18, 221–45.

Smith, N. D. 1974: Sedimentology and bar formation in the Upper Kicking Horse River, a braided outwash stream. *J. Geol.*, 82, 205–24.

Wertz, J. B. 1966: The flood cycle of ephemeral streams in south-western United States. *Ann. Assoc. Am. Geogr.*, 56, 598–633.

From Richards, K. (ed.) 1987
River Channels: Environment and Process.
Basil Blackwell

8

Mechanics of Flow and Sediment Transport in River Bends

William E. Dietrich

INTRODUCTION

In recent years, important progress has been made in the development of a general theory for flow, bed topography and planform evolution of river meanders. This has occurred despite a profound lack of detailed field observations with which to test not only the accuracy of predictions, but also and importantly, the assumptions upon which theory is constructed. The meander problem that has received the most advanced theoretical and experimental work is the analysis of the processes controlling equilibrium bed topography in a channel of a given planform. In this case, bed morphology remains essentially constant despite large fluxes of sediment and substantial shift of the flow through the bend. At every point on the bed, some overall balance of forces and sediment flux rates must obtain.

In river bends with heterogeneous mixtures of sediment sizes, a distinct sorting pattern often develops in which the coarser and finer bed particles trade position through the bend. The coarse particles shift from near the inside bank in the upstream part of the bend to near the outside bank downstream of the axis of the bend. The sorting process and its relationship to equilibrium bed morphology development has attracted sedimentologists concerned with reconstructing ancient rivers from depositional sequences, as well as geomorphologists and engineers seeking to explain observations of present-day rivers. This highly specified problem, then, has attracted researchers from many fields and has served as a common problem on which to hone observational and theoretical skills. These skills are in turn useful for the analysis of many different problems in river mechanics.

This chapter raises questions for both field-oriented scientists and theoreticians regarding what is known about the mechanics of flow and sediment transport

controlling bed morphology in river bends. Theory and observation have focused on channels with relatively small width-depth ratios. The first section of this chapter suggests that bed morphology varies with this aspect ratio and that more field and theoretical studies are needed on rivers with large width-depth ratios. The mechanics controlling flow fields in bends can perhaps be more clearly understood by examining separately the forces due to curvature change and bed topography variation through a bend. A simplified theory, containing elements of most flow models, can be employed to predict the velocity field through a bend and to illustrate effects of channel morphology on flow. An answer that is *close* to the correct answer is obtained with this simplest of approaches. For this reason, many theorists have made reasonably successful predictions. It is argued, however, that a complete but more complicated theory, without the use of adjustable parameters, is necessary to predict the form and behaviour of river bed morphology during stage change.

The chapter concludes with a discussion of the sediment transport processes controlling sorting and bed morphology in bends. Clearly the cross-stream bed slope and near-bed inward velocity in bends provide an ideal setting for strong segregation by size of bed materials, with the largest particles rolling downslope toward the pool and the fine particles being carried to the top of the bar by the inward flow. Also the outward shifting zone of maximum boundary shear stress through a bend must be balanced by cross-stream sediment fluxes. What is less clear is the relative importance to bed-morphology equilibrium of sediment suspension, bedform modification of flow and sediment transport direction, and grain size versus sediment flux adjustments to changing boundary shear stress fields. One case study is discussed where all these effects are evaluated and it is argued that some generality can be found through comparison with other less complete studies. More field studies are needed however, particularly in gravel-bedded and fine sand-bedded rivers.

PLANFORM AND BED TOPOGRAPHY

The beds of rivers are usually deformed into deep and shallow areas, often referred to as pools and riffles, respectively. Considerable research has been done to define the relationship between pool to pool or riffle-riffle spacing and channel width (e.g. Keller and Melhorn, 1973), or to investigate resistance and scour and fill tendencies with stage change (e.g. Lisle, 1979). Largely as a consequence of careful experimentation and observation in Japan (e.g. Kinoshita, 1961; Ikeda, 1984), there is a growing appreciation that the pool and riffle are part of a single bed-form, the bar unit (figure 8.1). In straight laboratory channels this bedform can develop into surprising regularity. As indicated in figure 8.1,

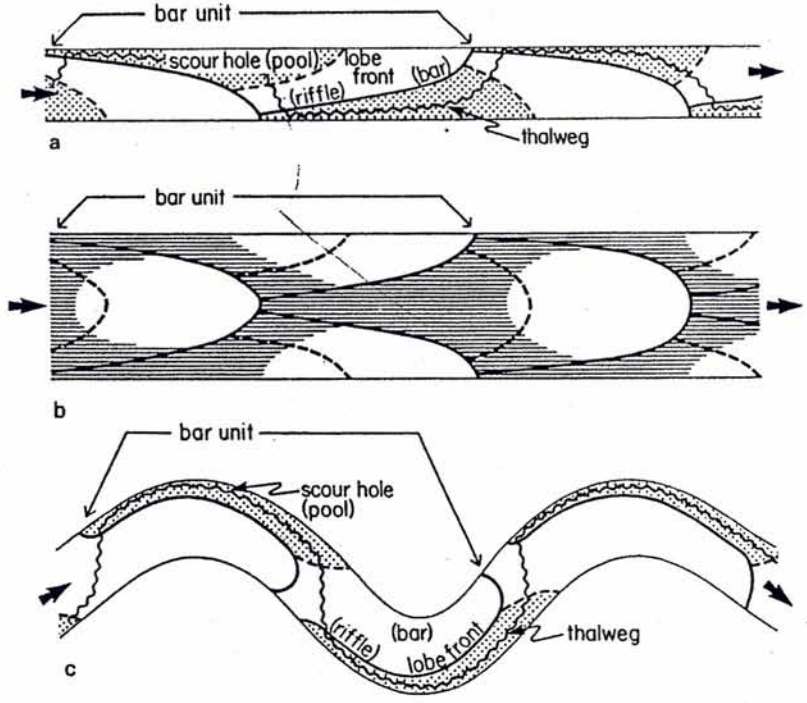

Figure 8.1 Bar unit morphology in straight (a), braided (b) and meandering channels (c). Bar unit consists of a narrow, deep scour hole (pool) that widens and shoals to an oblique lobe front (riffle and bar). The scour hole is shaded in a and c whereas the shading in b represents the low flow water level. Morphologic classification of bars based purely on their exposed portions fails to recognize the inherently three-dimensional nature of these large-scale features

the bedform consists of a downstream widening and shoaling scour hole (pool) terminating in an oblique shallow lobe front, the deepest portion of which is equivalent to the riffle. The shallowest portion of the bar is neither at the most downstream edge of the bar unit, nor along the closest bank; instead it is usually somewhat upstream of the bar front and toward the centre of the channel. When the bar pattern is repeated along opposite banks it is termed an alternate bar pattern; repeating as a mirror image across the channel is described as a row bar. It is argued by many (e.g. Kinoshita, 1961; Ikeda, 1984) that the row bar is the fundamental bed unit of braided channels, the shallowest portion of which in river sections may become stabilized by vegetation. In both the straight alternate-bar case and the braided channel, the bars migrate downstream.

In flume experiments or channelized reaches of rivers, alternate bar formation in channels with erodible banks typically leads to meandering (e.g. Friedkin,

1945; Lewin, 1976) and wrapping of the bar unit around the bend (figure 8.1c). In bends with small curvature, the bar will continue to migrate downstream (e.g. Hasegawa and Yamaoka, 1984), but with increasing curvature the bar will become fixed in the bend. Importantly, in a succession of low amplitude bends the pool of a bend is linked not to the point bar in the same bend, but to the downstream point bar (figure 8.1). In this case the oblique lobe front of the alternate bar becomes the point bar in the bend, retaining a strong obliquity to the banks. This obliquity causes the pool to widen downstream from the radius of curvature minimum. As in the alternate-bar case, there is a tendency in wide point bars for the shallowest portion to be detached from the inside bank, giving a humped cross-profile to the point-bar surface. High sinuosity bends with irregular planform and multiple point bars can be analysed in terms of alternating or repeating bar units within a single major bend, as will be described below.

The bar unit depicted in figure 8.1 is an idealization, clearly representative of features found in laboratory channels with uniform widths and smooth banks, but less obvious in natural rivers. As suggested by Bluck (chapter 7, this volume) other bar types may predominate on steep, gravel-bedded rivers. Most bar classifications (of which there are many - see Church and Jones, 1982 for an example, and Ferguson, chapter 6, this volume) are based only on the form of the lobe front exposed at low flow. Application of the bar-unit concept to natural rivers will require detailed topographic maps of the bed.

Point-bar morphology is greatly influenced by the width-depth ratio (w/d) in the bend. Extensive flume studies in straight channels have demonstrated that in narrow, deep channels alternate bar formation is suppressed. Although slope, Froude number and grain size influence this result somewhat, bars tend not to form below values of w/d of about ten. Brice (1984) labelled meandering rivers lacking point bars 'sinuous canaliforms'. Narrow, deep, curved channels nonetheless may form pools and bars with similar gross morphology to that depicted in figure 8.1 as a result of the curvature-induced secondary circulation, and spatial variations in the boundary shear stress field. Such bars have been called 'forced bars' by H. Ikeda (personal communication, 1985). For a bend of a given planform and radius of curvature to width ratio, however, the cross-channel profile varies significantly with the w/d. Figure 8.2a illustrates the cross-sectional form with varying w/d in the flume studied by Hooke (1974). Note that with increasing w/d, a broad, nearly flat surface formed out to the channel centreline. A similar result was obtained by Onishi (1972) in a flume in which he reduced the channel width by a factor of two by placing a wall along the centreline. Figure 8.2b shows the cross-channel profile change observed by Friedkin at the apex of an initial curved channel with w/d of seven as it widened to form a point bar and increase w/d to 53. Again, a broad, nearly flat bar surface formed over a significant portion of the profile.

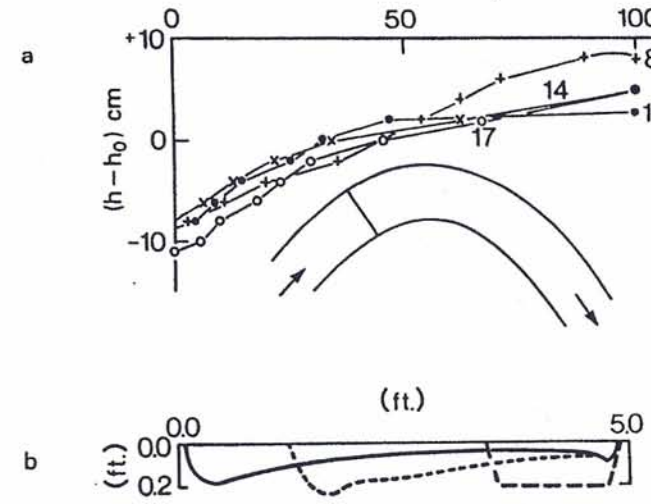

Figure 8.2 Variation in cross-channel profile in the meandering laboratory channel investigated by Hooke (1975) (a) and Friedkin (1945) (b). Vertical axis in a gives the difference between local and mean depth, h and h_0 respectively. Numbers to the right refer to the width to depth ratio of the experiment. In (b), successive lines represent progressive bar development through time along a cross-section. In both cases horizontal axis is the distance across the channel from the left bank.

The importance of w/d as a primary variable in channel form is demonstrated by the frequent use of this ratio as a principal parameter in distinguishing channel patterns (e.g. Parker, 1976; Fujita, 1982). In a channel with relatively erodible banks, alternate bar development will cause bank erosion, and the bar will widen, producing a strongly meandering thalweg in a channel whose banks show relatively low sinuosity. As Friedkin (1945) demonstrated there will be a tendency for the flow to cut off the widened bar along a chute channel once the bar has reached a certain width. Once cut off, a new bar will start to form again. The description provided by Friedkin is very similar to that given by Ferguson and Werritty (1983) for what they called a 'wandering gravel-bedded river'. In a sense this morphology and process represent the extreme bar response to high w/d without making the transition to row bars and braiding. It has also been proposed by Schumm (1963) that meander sinuosity is inversely proportional to w/d, but independent attempts to define a quantitative relationship suggest that it is an important but not dominant factor and that sinuosity depends on many variables (i.e. Chitale, 1970).

The width-depth ratio has received relatively little consideration in recent detailed studies of flow and sediment transport fields in river meanders. The necessity of working on relatively small rivers in order to collect accurate and

thorough data has resulted in a biasing of observations to stream channels with low w/d, typically 7 to 20 (e.g. Bridge and Jarvis, 1976; 1982; Dietrich et al., 1979; DeVriend and Geldof, 1983; Dietrich and Smith, 1983; 1984a; Thorne et al. 1985a). Presumably the main effect neglected by this biasing is the importance of the large relatively flat point-bar surface on flow and sediment transport processes in channels with large w/d. This point will be addressed later in this chapter.

Figure 8.3 shows the planform, low-flow channel (in black) and emergent point bars of three meandering reaches of relatively large rivers. Together these examples show the complexity of bar-planform relationships. Note that bankfull channel widths defined by the outer lines (as compared to the low-flow case in

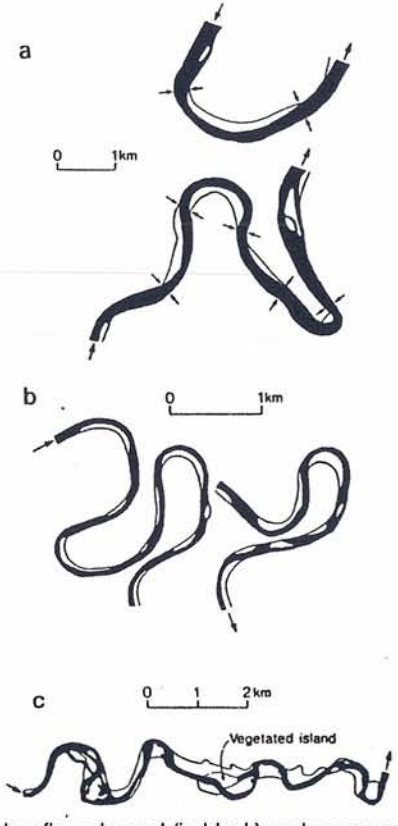

Figure 8.3 Planform, low-flow channel (in black) and emergent point bars (in white) on three meandering reaches of relatively large rivers. (a) Lower Wabash River studied by Jackson (1976); (b) Beatton River investigated by Nanson and Hickin (1983); (c) Lower Babbage River studied by Forbes (1983). Rivers in (a) and (b) are sand-bedded, whereas (c) is gravel-bedded

black) are systematically narrower in the crossings than in the bends (note arrows at crossings in figure 8.3a). Few of the meanders have smoothly varying curvature and parallel banks; instead curvature increases abruptly downstream of the crossing, and then tends to diminish downstream. Large amplitude bends tend to have a second curvature maximum in the downstream ends before the next crossing. Several authors have argued that asymmetry is typical of large bends (see review in Hooke, 1984). Hasegawa (1983), for example, found that a modified 'sine-generated' curve equation which produced an asymmetric meander pathline with two radii of curvature minima (like figure 8.3b) best fits planforms of several rivers in Japan (see summary in Yamaoka and Hasegawa, 1984).

In figure 8.3, the white zones recording the shallow point-bar top (at bankfull stage) distinctly wrap around the convex bank and are elongated in the downstream direction. In the most sinuous meanders (figure 8.3b) multiple bars

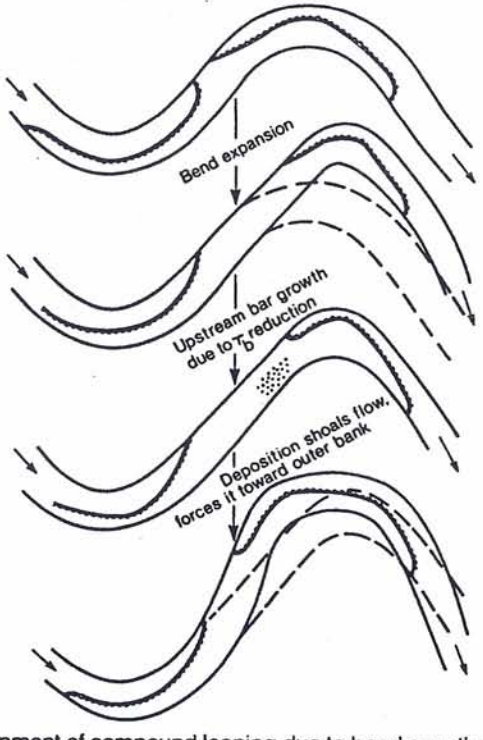

Figure 8.4 Development of compound looping due to bend growth relative to upstream bend. The sequence of channel paths illustrates the hypothesis that as the bend expands, there should be a tendency for boundary shear-stress reduction near the bend entrance due to lengthening of the channel path from apex to apex in successive bends. Reduced boundary shear stress would lead to deposition, bar growth, shoaling induced outward deflection of the flow towards the outer bank and compound looping.

have formed within a single complex bend. Approximately three complete asymmetric bends are represented in each of the two reaches. Within these reaches the average bar spacing in channel widths is eight (left channel) and five (right channel), and a near-alternate bar sequence is present in the downstream convex portion of the left channel. Keller (1972) and Hooke and Harvey (1983) suggest that a path-length dependent bar instability, like that responsible for alternate bar formation, leads to multiple bars in the limbs (Keller) or compound looping (Hooke and Harvey), although the fluid mechanics responsible for this instability in a curved flow are not described. One mechanism is illustrated in figure 8.4, whereby growth of the downstream bend results in a systematic reduction in the boundary shear stress responsible for sediment transport along the inside bank of the bend. This shear stress reduction leads to bar growth, deflection of flow toward the outer bank and compound looping (*sensu* Brice, 1984) of the bend. Perhaps another important mechanism is that proposed by Struiksma et al. (1985) in which the rapid radius of curvature change from the crossing into the bend induces a damped periodic response in the resulting bed topography in a bend. The development of a secondary circulation in the pool and outward shift of the high-velocity core causes scour along the outer bank; in response, the pool deepens, forcing net cross-stream sediment transport across the bar into it. In effect, in the upstream part of the bend, the pool over-deepens to produce a steep lateral bed slope and a net cross-stream sediment transport, a process Struiksma et al. (1985) refer to as an 'overshoot effect'. Further downstream, as the flow adjusts to an imposed constant channel curvature, the pool depth will shoal and then again deepen to a lesser extent, forming a secondary maximum depth. Although the secondary pool maximum is much less than the first, this oscillatory behaviour may contribute to development of an additional bar within a long bend. According to Struiksma et al. (1985) a similar damped periodic behaviour will result at the bend exit and into the downstream crossing. Hence their model would also predict bar instability in long crossings. It is not as yet established, however, that this theory has applications to natural river meanders, which may have much greater frictional damping than laboratory channels.

Point-bar formation is also controlled by local bank resistance and the strength of channel curvature, the latter of which is usually characterized by the diminishing ratio of the radius of curvature to channel width (r_c/w). Along the same channel, deeper pools will tend to develop against more resistant bank material (Friedkin, 1945) and in bends with smaller r_c/w. Sufficiently large bank obstruction relative to the channel size will turn the flow, producing a forced bar with an oblique bar face similar to that in the freely meandering case (Lisle, 1986). Bank obstructions may also 'stall' a meandering loop (Reid, 1984) by preventing bank erosion, such that the upstream bend can overtake it. This

causes the upstream inside bank to erode faster than the outside one, resulting in bank migration away from the concave outside bank and deposition of a bar where once the pool lay.

In summary, point bars in meandering rivers are equivalent to the lobe fronts in alternate bars. In wide, shallow channels the bar top is relatively flat in the zone of curvature maximum and may extend well across the channel. In narrow, deep channels the point-bar development is suppressed, the flat bar top may be absent and in rivers that otherwise would not produce alternate bars in straight reaches, channel curvature will produce a 'forced bar'. The break in slope from the bar top to the face into the pool tends to cut obliquely across the channel, extending from close to the outside bank in the radius of curvature minimum to the inside bank further downstream. River meanders typically have distinct curvature maxima, often having more than one in large amplitude bends. These maxima may be a consequence of bar development, or may be responsible for bar formation, depending on their origins. Bend asymmetry is common in some rivers, perhaps more often skewed with an elongated downstream limb, and in such bends multiple bars and downstream-elongated bars are common. This description provides a morphologic framework for investigation of flow through meanders.

FLOW AND BOUNDARY SHEAR STRESS IN RIVER BENDS

Flow fields in rivers are controlled in large part by the resultant of forces arising from channel curvature, changes in curvature and gradients in bed topography. The flow response to channel planform and topography in turn dictates the boundary shear-stress field which controls the transport of sediment - hence for sediment transport studies of bars, an understanding of the flow fields in bends is essential. Here I briefly review observations and theory for flow in meandering streams in order to discuss sediment transport processes. Detailed discussions and other references can be found in Dietrich and Smith (1984a), Elliott (1984), Hasegawa and Yamaoka (1984) and Smith and McLean (1984).

Curvature effects

Channel curvature forces major adjustments in flow patterns. It is well understood that curvature results in a centrifugal force acting in the cross-channel direction. This force is counter-balanced primarily by the cross-stream tilt of the free surface, which causes a cross-stream pressure gradient force. This balance holds only in the vertically-averaged flow because the surface velocity is much faster than the near-bed velocity due to boundary resistance. The slow near-bed flow

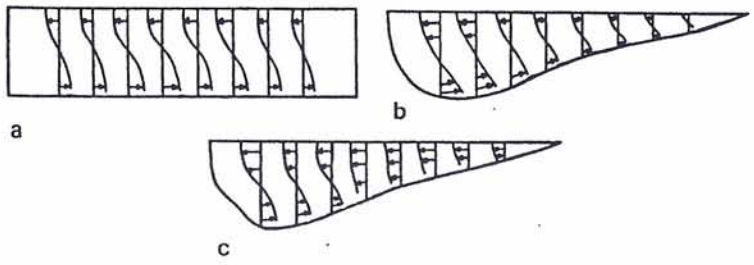

Figure 8.5 (a) secondary circulation in a rectangular channel of constant curvature; (b) the assumed pattern of secondary circulation in bends which may only develop in regions well downstream of radius of curvature minima; (c) the observed pattern in the upstream end of a bend with well developed bar and pool topography. Lines not continued to streambed because of inadequate space to show that they must curve back to zero on the vertical

is turned inward whereas the high centrifugal force of the near surface flow carries it outward against the opposing pressure-gradient force; the net effect is a spiral-like motion, sometimes described as helicoidal flow (figure 8.5).

This rotational motion, a secondary circulation relative to the main flow direction, is usually described as the main effect of curvature on flow, but there is another, very important consequence of curvature: the tilting of the water surface alters the downstream slope of the water surface, generating large cross-stream variation in the downstream boundary shear stress and velocity fields. Figure 8.6 illustrates channel curvature and bed topography effects on flow. Across the top of figure 8.6 three equations are written that in turn express the principal cross-stream and downstream force components on the flow and the dependence of the local downstream slope on water surface elevation change and varying travel distances due to curvature. The equations are written using a co-ordinate system that follows the channel centreline (e.g. Dietrich and Smith, 1983; Smith and McLean, 1984) in which s points downstream parallel to the centreline, z points nearly vertical and n, the cross-stream axis, is positive toward the left bank. The scale factors (metric coefficients) for derivatives with respect to the cross-stream and vertical co-ordinates are unity, but the one associated with the downstream coordinate is $1-n/R=1-N$, *where* R is the local radius of curvature of the centreline. This scale factor compares an arc length measured along the channel centreline to that measured along any other line of constant n.

The first equation is derived from the force balance between the cross-stream centrifugal force term and the cross-stream pressure gradient term

$$\frac{\varrho<u_s^2>h}{(1-N)R} = -\varrho g h \frac{\partial E}{\partial n} \qquad (8.1)$$

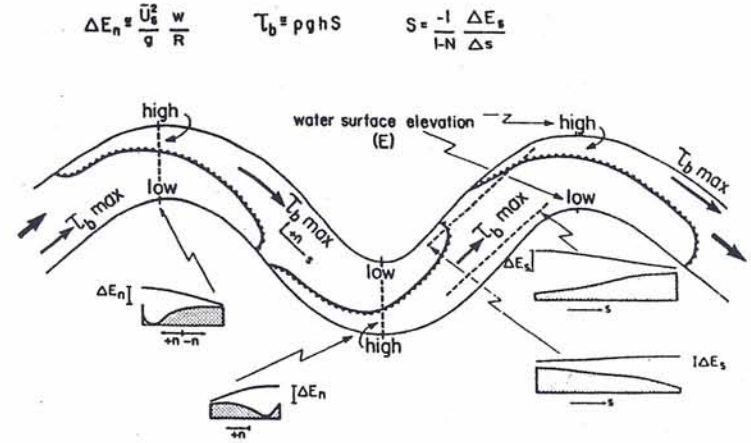

Figure 8.6 Channel curvature and bed topography effects on the boundary shear stress field. Break in bar slopes indicated by serrated edge. Curvature induces centrifugal forces and changes in water-surface elevation that in a meandering reach forces skewing of the downstream boundary shear stress fields. Bar-pool topography causes the maximum boundary shear-stress zone to shift outward further upstream than would occur due to curvature alone. Equations across the top are explained in the text

where $<u_s>$ is the vertically averaged downstream component of velocity, h is the depth of flow, g is the gravitational acceleration, ϱ is the fluid density, and E is the elevation of the water surface. Approximate integration of (8.1) across the channel yields the first equation in figure 8.6, in which $\overline{U}_s$ is the cross-sectionally averaged downstream mean velocity, w is the flow width and ΔE_n is the total water surface elevation change from the inside to the outside of the channel. Although incomplete (e.g. Yen and Yen, 1971; Dietrich and Smith, 1983; Smith and McLean, 1984), equation 8.1 includes the most important terms.

In a channel with smoothly varying curvature and uniform width, as depicted in figure 8.6, ΔE_n will increase into the area of radius of curvature minimum, decrease to zero in the crossing and increase again, but in an opposite direction, into the next bend downstream. Consequently the water surface will rise and become relatively high along the concave outer bank, and drop along the convex ones (figure 8.6). This has an important effect on the boundary shear stress and velocity fields.

In steady uniform flow the local downstream boundary shear stress, τ_b, can be approximated as

$$\tau_b = -\frac{\varrho g h}{(1-N)} \frac{\partial E}{\partial s} \qquad (8.2)$$

Strictly this equation is accurate only for channels with constant curvature and bed topography (e.g. Dietrich and Smith, 1983). For the case depicted in figure 8.6, if the bars were absent and instead the cross-sections were the same throughout, equation (8.2) should be reasonably accurate except in areas of rapid curvature change. In this case, then, variations in flow depth would not contribute to the changes in the boundary shear-stress field. Nonetheless, large changes would develop due to the effect of centrifugal forces on water-surface topography. As shown in figure 8.6, the rising of the water surface near the concave bank of the upstream bend and the dropping downstream along the convex one will generate a locally steep downstream water-surface slope, hence a zone of maximum boundary shear stress. On the opposite side of the channel, the water surface will either drop very little to the downstream high along the outer bank or it may (as shown in figure 8.6) rise, in which case the water-surface slope is reversed and according to equation (8.2) the boundary shear stress would be negative. Hence just the effect of centrifugal forces on the flow through a meander should tend to produce a zone of maximum boundary shear stress (and maximum average velocity) that shifts from near the inside upstream bank to near the outside downstream one through the zone of radius of curvature minimum (figure 8.6). In the special case of uniform bed topography, such as the rectangular or trapezoidal shapes often used in experiments, and a curved section of constant curvature joined by straight reaches, the boundary shear-stress maximum will develop along the inner convex bank and will not shift toward the outer one until the downstream end of the bend where the radius of curvature changes from a small constant value to infinite (Dietrich and Smith, 1983; Smith and McLean, 1984).

To summarize, channel curvature results in centrifugal forces which lead to a secondary circulation. Water surface slope changes due to curvature result in the development of a zone of maximum boundary shear stress near the convex inside bank. Curvature change, from a large value in the bend to zero at the crossing to a large value of opposite sign downstream, results in cross-stream shifting of the zone of maximum boundary shear stress. Bar and pool topography, which will be discussed next, alters the orientation of the near-bed velocity, increases the cross-stream variation in boundary shear stress field and causes rapid shifting of the maximum across the channel.

Bed topography effects in straight and curved channels

Laboratory (Hasegawa, 1983; Ikeda, 1984) and field (Leopold, 1982) measurements, in addition to theoretical investigations (Smith and McLean, 1984), show that alternate bars in straight channels strongly influence the cross-stream distribution of the mean velocity and the near-bed velocity orientation.

Figure 8.7 illustrates the vertically-averaged velocity field in a laboratory channel with self-formed alternate bars. As shown previously in figure 8.1, the bar unit will be deepest at its upstream end and shoal progressively downstream. Note that a complete bar unit is not shown in figure 8.7, only the downstream half of one and the upstream portion of the next unit. A minimum depth downstream typically occurs somewhat upstream of the lobe front (indicated by serrated edges in figure 8.7) and towards the centre of the channel. The flow field depicted in figure 8.7 graphically demonstrates that shoaling of the flow in the downstream direction from pool to lobe front generates a net cross-stream discharge toward the adjacent pool. The vectors representing vertically-averaged velocity are oriented strongly across the channel over much of the downstream outer portion of the bar unit. In addition, the position of the maximum velocity (as indicated by arrows) shifts abruptly across the channel. In effect, the flow finds it 'easier' to go around the bar rather than directly over it. This is due in part to the change in the downstream pressure gradient (right side of equation (8.2)) with depth variation, and in part to convective accelerations due to the downstream gradients in flow depth (see Dietrich and Smith, 1983, p. 1174 and their figure 3 for further discussion).

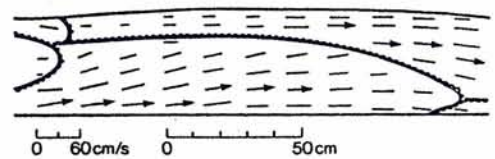

Figure 8.7 Vertically averaged velocity field over self-formed alternate bars in a laboratory flume (modified from Ikeda, 1984). Only downstream end of one bar and upstream end of next bar unit shown. Arrows indicate position of maximum velocity. Triangular edging points toward deep water. Minimum depth probably occurred at third to last section over central bar

In curved channels with well developed bars, topographically induced forces arise that strongly influence the boundary shear stress and velocity fields. As in the alternate-bar case, shoaling of the flow will tend to turn the flow toward the pool, causing significant net cross-stream discharge. Consequently, where shoaling is strong, the vertically averaged velocity vector over the bar will point toward the pool, and although secondary circulation must still occur, the near bed velocity and resulting boundary shear stress will be oriented towards the outer bank as well. Hence, bar growth into the flow will radically alter the near bed cross-stream velocity pattern. This conclusion is supported by numerous flume studies analysed by Dietrich and Smith (1983), by a recent extensive laboratory investigation by Hasegawa (1983) (see Hasegawa and Yamaoka, 1984

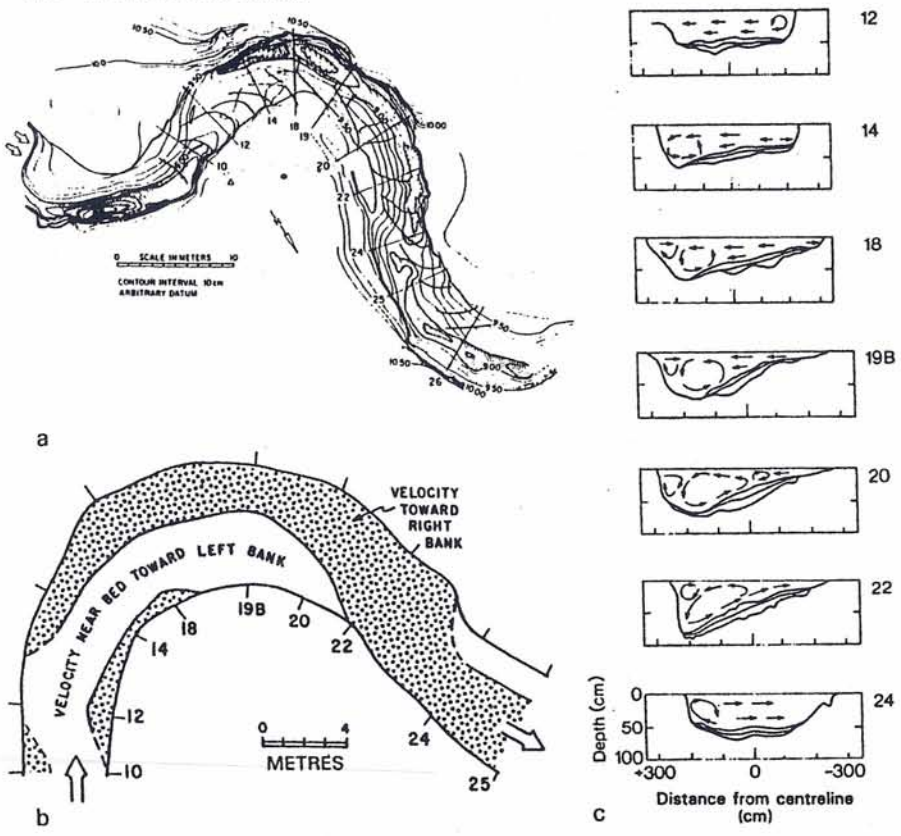

Figure 8.8 (a) bed topography; (b) near-bed velocity orientation; (c) cross-stream velocity field in Muddy Creek, a small sand-bedded stream. Note the evolution of the cross-stream velocity from outward through water column (12), to progressive development of helical motion with inward near-bed velocity over the pool (14-22), to outward at the entrance of next bend downstream. Arrows are qualitative interpretations of the cross-stream velocity field reported in Dietrich and Smith (1983, figure 11)

and Yamaoka and Hasegawa, 1984), by detailed field studies and re-analysis of previously published field data (Dietrich and Smith, 1983) and by new field studies (Thorne et al., 1985a; 1985b).

Figure 8.8 shows the pattern of bed topography, cross-stream velocity field and near-bed velocity orientation in a small, sand-bedded river meander. The site and field methods are described in previous publications (Dietrich et al., 1979; 1984; Dietrich and Smith, 1983, 1984a, 1984b). In brief, Muddy Creek receives nearly constant irrigation outflow each spring which, in combination with an adequate supply of sediment from erodible banks of sandy alluvial

deposits, results in the formation of a bed topography in equilibrium with flow. Importantly, direct measurement of bed topography during field experiments and in successive years at the same discharge clearly demonstrates a well-defined equilibrium bed topography. Hence observations could be made under flume-like conditions that defined a mutual adjustment between flow and bed topography to an equilibrium condition. This analysis is important because the effect of bed topography on flow varies strongly as the stage deviates from that in equilibrium with the bed.

In the Muddy Creek bend (figure 8.8), width-depth ratio increases from 10 in the crossings (just upstream of sections 12 and 24) to 17 in the centre of the bend (section 19) and the radius of curvature-width ratio is about 1.5 for the central part of the bend. The central bend had an approximately constant radius of curvature from section 14 to section 20 (Dietrich and Smith, 1983, figure 9) and most of the curvature change occurred at the entrance and exit of the bend over a distance of about one channel width.

The cross-stream velocity field depicted in figure 8.8 shows that strong outward velocity (and net discharge) develops in the crossing (sections 12 and 24) downstream of a bend. Through the crossing and into the centre of the bend, the discharge vector between successive sections is oriented 4° to 7° toward the outer bank relative to the channel centreline path. The spiral motion in the cross-stream plane forms as the pool develops and expands across the channel progressively (section 14 to 22). Shoaling over the bar along the inside bank forces the flow into the pool and the cross-stream velocity is oriented toward the pool throughout the water column. The near-bed velocity direction is towards the pool in the upstream part of the bend where the flow is shoaling; downstream of section 19B the bar deepens and the helical motion expands across the channel. Shoaling, bank effects (which lead to an opposite spiral near the surface and over the upsloping bank), and possibly lee effects of the point bar along the inside bank, cause the zone of spiral motion with outward flow near the surface and inward flow near the bed to be confined to the deepest 20 to 30 per cent of the channel cross-section. Downstream of section 20, weak net cross-stream discharge towards the downstream end of the pool develops as the pool width increases.

Based on available field and laboratory measurements in the references cited above, a sketch of the flow pattern in equilibrium with the bed topography in bends with well developed bars can be constructed (figure 8.9). Two cases are shown, a low amplitude bend with strong curvature and a similar bend with a long downstream 'tail' of nearly constant curvature. Of course many other combinations occur, but these figures illustrate several important aspects of flow in bends. The lobe front is indicated with a serrated edge and the thalweg with a dashed line. The bar top at low flow is shaded in order to relate this pattern

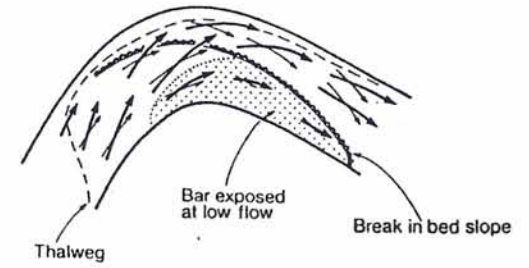

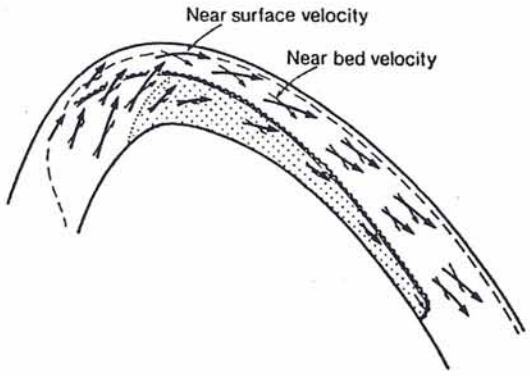

Figure 8.9 Flow field in equilibrium with bed topography in bends with well developed bars. Note shoaling-induced outward flow upstream of radius of curvature minimum, and downstream-growing region of spiral motion with inward near-bed velocity vector. Stippled area represents exposed portion of bar unit during low flow

to the low-stage appearance more commonly seen in rivers. Two arrows, a heavy larger one over a shorter one, represent the surface and near-bed velocity, respectively. The representation is not meant to be quantitative and compromises are made in order to depict important effects. Nonetheless the length and orientation of the arrow crudely represent the corresponding velocity vector.

There are several important features of the illustration. Firstly, in the upstream part of the bend as the flow is adjusting to the sudden reduction in radius of curvature, the shoaling over the bar and deepening over the pool lead to outward deflection of the flow toward the pool. The curvature and consequent centrifugal force and counteracting cross-stream pressure gradient still result in a secondary circulation, but the plane of the circulation is curved and not oriented normal to the channel path. Hence surface velocity vectors are oriented more toward the outer bank than near-bed vectors, but these bottom vectors are also pointed slightly outward toward the pool. Secondly, this pattern differs substantially

over the pool (toward the concave bank from the lobe front) and over the bar downstream of its maximum height (which is typically in the zone of radius of curvature minimum). In the pool the near-bed velocity is oriented strongly inward, either parallel to or slightly up the point-bar face of the lobe front. A secondary circulation, the axis of which is oriented approximately parallel to the channel path, develops. The pool width expands downstream and correspondingly, the zone of spiral motion generating inward near-bed velocities increases. Figure 8.5c shows a typical cross-stream velocity pattern in the upstream part of the bend. In addition, the velocity increases downstream through the pool. Downstream of the maximum bar height and the radius of curvature minimum, the velocity rapidly decreases near the inside bank, and weak inward near-bed velocities may develop. Thirdly, if a long reach of constant curvature develops, then the flow adjustments to channel path and topographic changes may be nearly complete and a zone of nearly uniform flow with a high velocity region near the outer bank and a constant spiral motion (figure 8.5b) may develop.

Figure 8.9 is in contrast to the surface flow pattern proposed by Hey and Thorne (1975), and illustrated in several texts (Richards, 1982; Knighton, 1984). At flow stages in equilibrium with the bed, the surface flow is not as strongly oriented across the channel as depicted in their drawing. The cross-stream velocity field must include a shoaling-induced outward flow over the bar if the bar is extended well up into the flow. Dual secondary cells are not clearly present in the crossings of natural channels; apparently one cell does not grow over another one. Finally the cell of opposite motion to the main one in the bend, which they correctly point out as developing along the outer bank, appears to be confined to a region very close to the bank.

It is commonly assumed in modelling of flow and sediment transport processes in bends that over a significant portion of the bend the flow becomes 'fully developed' (e.g. Yen, 1965; Jackson, 1976), meaning that the flow field and bed topography remain constant downstream through the bend. As Jackson (1976) correctly noted, most natural river channels vary too much in form and their bends are too short, in terms of response to imposed changes, for fully developed conditions to obtain. Even in long laboratory channels of constant curvature as mentioned above, it has been observed that a uniform downstream pool depth does not develop (i.e. Odgaard, 1981; Struiksma et al., 1985). Once the high velocity core has crossed to the outer bank, however, a secondary downstream curvature minimum and local bar emergence may have a smaller but not insignificant influence on the flow, as is suggested by the laboratory experiments of Hasegawa (Hasegawa and Yamaoka, 1984; Yamaoka and Hasegawa, 1984).

The pattern of flow in bends is strongly stage dependent. Without topographic adjustments due to sediment transport, an increase in stage away from the equilibrium condition shown in figure 8.9 will reduce the shoaling effect, and

increase the near-bed inward component of velocity, allowing an inward component of flow to develop over the bar top. This is perhaps most clearly demonstrated in the theoretical calculations of Smith and McLean (1984, figure 5) in which the effect of increasing bar height relative to flow depth was investigated. A stage drop without topographic adjustment will greatly increase the shoaling effect and the flow downstream in the bend will be confined to the pool exposing the downstream bar top. If the bed remains mobile during a stage drop, as it can in sand-bedded channels, topographic adjustments will occur that reduce the erosive effect of strongly diverging boundary shear stress caused by shoaling. Equilibrium bed morphology can develop at any stage as long as the discharge remains sufficiently constant and the bed remains mobile.

The dependence of flow patterns on stage, as a result of bed immobility or delayed topographic response of a mobile bed, emphasizes the great need to establish whether the flow is in equilibrium with the bed topography when studying flow patterns in channels. Regrettably, most studies have not considered this problem carefully. Imbrication studies on exposed gravel bars during low flow will not give a reliable indication of high-flow patterns and sediment transport directions (Aristov, unpublished data). Although the gravel becomes relatively immobile as the stage drops below that capable of shaping the bed, the individual particles can still be rotated in their resting pockets and imbricated by the flow. Imbrication should therefore express strong shoaling effects with inferred directions oriented toward the outer bank, as is commonly seen on exposed bars.

Three other sand-bedded rivers (besides Muddy Creek) where flow patterns have been reported are the South Esk River (Bridge and Jarvis, 1982), the Fall River (Thorne et al., 1985a; 1985b) and the River Dommel (Van Alphen et al., 1984). In all three cases, bed topography was not clearly shown to be in equilibrium with the imposed flow. The most extensive data, those of Bridge and Jarvis (1982), are reported for several stages. Comparison of cross-sections, particularly in the upstream part of the bend, shows no change in bed topography over a broad range of stages. The highest stage data were collected, apparently immediately after a period of about a month of low flow. It is suggested that the data of Bridge and Jarvis record a high flow over a low-flow bed topography. As Dietrich and Smith (1983) demonstrated, the secondary flow observations of Bridge and Jarvis also do not conform to conservation of mass requirements.

Field measurements of velocity vectors must be done with reference to some cross-section orientation. Two choices for cross-section orientation are: perpendicular to the channel walls if the channel width and curvature are constant (as in the flume case), and parallel to the orientation required by continuity (Dietrich and Smith, 1983). In essence this latter requirement states that velocity or topographic changes between successive sections that alter the local discharge

per unit width must be compensated by a cross-stream discharge of water. Thus, for example, at the entrance to the bend the flow often rapidly shoals downstream over the bar, but the average velocity varies little, hence net discharge between successive sections towards the pool must occur. Cross-sections must be oriented such that the measured cross-stream discharge matches that required by this continuity constraint. As virtually no stream has constant width and curvature, the continuity requirement must be employed. Smith and McLean (1984) showed that the vertically averaged continuity equation for steady flow is (in the orthogonal curvilinear co-ordinate system in figure 8.6).

$$\frac{1}{1-N}\frac{\partial <u_s> h}{\partial s} - \frac{<u_n> h}{(1-N)R} + \frac{\partial <u_n> h}{\partial n} = 0 \qquad (8.3)$$

and they solved it for $<u_n>h$, the local cross-stream discharge per unit width, to get

$$<u_n>h = -\frac{1}{1-N}\int_{-w/2}^{n}\frac{\partial <u_s> h}{\partial s}\,dn \qquad (8.4)$$

Here $<u_n>$ and $<u_s>$ are the cross-stream and downstream vertically averaged velocity, respectively; $-w/2$ is the right-bank position of a channel with a width w. Equation (8.4) can be used in a simple procedure to determine the correct cross-sectional orientation for calculation of the cross-stream velocity field. Field selection of section orientation is used to compute the down-stream and cross-stream components of the vertically averaged velocity. The total cross-stream discharge of water, Q_{nw}, required by continuity can be computed from equation (8.4) by integration from bank to bank:

$$Q_{nw} = \int_{-w/2}^{w/2} <u_n> h\,dn = \int_{-w/2}^{w/2}\left[\frac{-1}{1-N}\int_{-w/2}^{n}\frac{\partial <u_s> h}{\partial s}\,dn\right] dn \qquad (8.5)$$

The average direction of flow, θ_w between successive sections with an average downstream discharge Q_{sw} is

$$\theta_w = \tan^{-1} Q_{nw}/Q_{sw} \qquad (8.6)$$

This angle can be compared with the angle computed from the observed cross-stream velocity components defined relative to the field-selected orientation of the section. The observed angle can then be corrected to give the computed value. This correction is typically small if the field orientation is carefully

selected and iteration, correcting the downstream velocity and repeating the procedure, appears to be unnecessary.

The only other river besides Muddy Creek in which the orientation of the cross-sections were apparently correctly oriented following the above procedure is the Fall River (Thorne and Rais, 1984; Thorne et al., 1985a; 1985b). The results for this river are not easily interpreted, however, because, as mentioned above, the bed topography was not demonstrated to be in equilibrium at the stages studied. Furthermore, and more confusing, the results reported in Thorne et al. (1985a), in which they conclude that one bend shows the shoaling effects of outward flow over the bar and an adjacent one does not, do not appear to agree with the basic data shown in a separate report (Thorne et al., 1985b).

As a final comment, looking back at figure 8.6, it can be seen that an additional effect of well developed bar-pool topography in a bend is to cause a rapid shifting of the zone of maximum boundary shear stress into the downstream end of the pool (where hS in equation (8.2) is large) and to reduce the magnitude of the boundary shear stress over the bar downstream of the radius of curvature minimum (where hS in equation (8.2) is small). Similarly, the zone of high velocity would shift rapidly across the channel. The crossing into the pool may be shifted downstream by inertia of the fluid as it crosses over the steeply sloping boundary and locally reduces the vertical velocity gradient (Dietrich et al., 1979, p. 310). In the following, inertial forces will be discussed more quantitatively.

THEORY FOR FLOW IN BENDS

The number of mathematical theories for predicting flow in bends greatly exceeds the number of careful field studies with which to test the theories. There is little sign that the production of new theories will slow down, but unfortunately few detailed investigations of field sites are being conducted and only a small range of channel shapes have been examined. Hence, with the present paucity of detailed field data it is difficult to test the generality of available theories. On the other hand, due to the relatively simple nature of the gross features of flow through a bend, models that include the major forces acting on the flow are going to appear to be fairly successful. However, accurate portrayal of such details of the flow pattern as the outward flow over the bar, though rarely tested for in flow models, strongly affects the usefulness of the model in geomorphic and sedimentologic studies of river bends.

In general, flow models have tended to become increasingly more complex as simplifying assumptions have been shown to be invalid. All models must start with the equation of motion for a general fluid flow:

$$\varrho \frac{d\mathbf{u}}{dt} = -\nabla p + \nabla \cdot \bar{\tau} - \varrho \mathbf{g} \qquad (8.7)$$

where u is the velocity vector; t and ϱ represent time and density respectively; p is pressure; $\bar{\tau}$ is the deviatoric (non-isotropic stress); and g is gravitational acceleration. Equation (8.7) has usually been written in cylindrical co-ordinates and through various assumptions simplified to a series of force balances in each of the three dimensions (i.e. Rozovskii, 1957; Yen, 1965). Natural rivers have continuously varying curvature and a more useful co-ordinate system is that proposed by Smith and McLean (1984) and depicted in figure 8.6. Smith and McLean show in an appendix to their paper the complete derivation of the full equations in the n, s and z co-ordinates. By vertically integrating these equations and employing reasonable arguments for the relative size of terms and discarding the much smaller ones, Smith and McLean arrived at the following important force balance equations:

$$(\tau_{zs})_b = \frac{-\varrho g h}{1-N}\frac{\partial E}{\partial s} - \varrho \frac{1}{1-N}\frac{\partial}{\partial s} <u_s^2> h$$
$$- \varrho \frac{\partial}{\partial n} <u_s u_n> h + \frac{2\varrho <u_s u_n> h}{(1-N)R} \qquad (8.8)$$

$$(\tau_{zn})_b = -\varrho g h \frac{\partial E}{\partial n} - \varrho \frac{<u_s^2> h}{(1-N)R} - \varrho \frac{1}{1-N}\frac{\partial}{\partial s} <u_s u_n> h$$
$$- \varrho \frac{\partial}{\partial n} <u_n^2> h + \frac{\varrho <u_n^2> h}{(1-N)R} \qquad (8.9)$$

All the terms are the same as defined above and $(\tau_{zs})_b$ and $(\tau_{zn})_b$ are the downstream and cross-stream components of boundary shear stress. Comparisons of equations (8.8) with (8.2) shows that in addition to the pressure gradient force, two momentum-change terms, associated with downstream $\left[\frac{\partial h}{\partial s}\right]$ and cross-stream $\left[\frac{\partial h}{\partial n}\right]$ bed slopes, and a force due to channel curvature are included in the balance with the downstream component of the boundary shear stress. Comparison of equations (8.9) with (8.1) reveals that the simple force balance represented by equation (8.1) neglects the effects of boundary friction (in generating a cross-stream component of the boundary shear stress), change in momentum terms associated with bed topography and an additional centrifugal acceleration term associated with the cross-stream component of flow. In

equations (8.8) and (8.9) the momentum change terms are largely a consequence of the downstream and cross-stream bed slopes, hence are referred to as topographically induced convective accelerations. As suggested in the discussion of figure 8.6 and as will be shown below, equations (8.1) and (8.2) can be used to explain the basic vertically averaged flow pattern in bends. Although only limited data are available from laboratory flumes (Yen and Yen, 1971) and from field studies (Dietrich and Smith, 1983) which are sufficient to calculate the terms in equations (8.8) and (8.9), both quoted experiments demonstrate that the convective acceleration terms, i.e. those forces arising from change in momentum downstream and across the stream, are large and must be included in an accurate determination of the force-balance and resulting boundary shear-stress fields. Dietrich and Smith, however, point out that very close spacing of cross-sections and highly accurate measurement of flow fields and water topography are required to evaluate correctly the terms in equations (8.8) and (8.9); this is very difficult to achieve in natural rivers (see also comments by Sigenthaler and Shen, 1984). They also note that in both their data and those of Yen and Yen, there appears to be a tendency for the momentum change terms to be of opposite sign. This explains why equations (8.1) and (8.2) yield approximately correct results. Nonetheless, theoretical investigations (Kalkwijk and DeVriend, 1980; Smith and McLean, 1984) have shown it essential to include all the terms in equations (8.8) and (8.9) in order to predict with reasonable accuracy the flow and boundary shear-stress field in bends with bar and pool topography. Analysis of these and other theories is beyond the scope of this chapter, but in order to appreciate the mechanics of flow in bends and to understand why many less complete models give approximately correct solutions, a simple analysis is performed below.

Approximation of flow in a bend

The simplest downstream force balance for channel flow is the steady, uniform flow approximation, equation 8.2, rewritten here by noting that τ_b equals $(\tau_{zs})_b$ in equation 8:

$$(\tau_{zs})_b = -\frac{1}{1-N}\,\varrho g h\,\frac{\partial E}{\partial s} \tag{8.10}$$

The water surface elevation at any point in the channel can be related to the centreline elevation, E_o, through the cross-stream gradient of the surface,

$$E = E_o + n\,\frac{\partial E}{\partial n} \tag{8.11}$$

hence,

$$\frac{\partial E}{\partial s} = \frac{\partial E_o}{\partial s} + n\,\frac{\partial}{\partial s}\left[\frac{\partial E}{\partial n}\right] \tag{8.12}$$

Rearrangement of the dominant cross-stream force balance, equation (8.1), to

$$\frac{\partial E}{\partial n} = -\frac{<u_s>^2}{g(1-N)R} \tag{8.13}$$

and substitution of equations (8.12) and (8.13) into (8.10) yields

$$(\tau_{zs})_b = -\frac{\varrho g h}{(1-N)}\frac{\partial E_o}{\partial s} + \frac{\varrho n h}{(1-N)^2}\frac{\partial}{\partial s}\left[\frac{<u_s>^2}{R}\right] \tag{8.14}$$

Equation (8.14) shows how the boundary shear-stress field will vary with the downstream component of the horizontal pressure gradient as defined by the centreline slope and with the centrifugal force-induced tilting of the water surface. Recall that in this co-ordinate system, n is negative toward the right bank. In the case in which the right bank is the convex inside of the bend, R is also negative. Hence near the inside bank as R decreases into the bend $\frac{\partial}{\partial s}\frac{1}{R}$ will be negative, n will be negative and the second term will be positive increasing the local boundary shear stress relative to that of the centreline. Over the pool near the outside bank where n is positive the second term will reduce the local boundary shear stress. Downstream of the curvature minimum, where $\frac{\partial}{\partial s}\frac{1}{R}$ is positive the opposite effect will occur and consequently the boundary shear stress should be high in the pool and low over the point bar. The depth term, h, should tend to make the boundary shear stress greatest in deepest water but this is counteracted by the $(1-N)$ term, the metric coefficient that accounts for the shorter distance along the inside bank than along the outside one, and by the curvature changes described above. The contribution from $\frac{\partial <u_s>^2}{\partial s}$ cannot be inferred as easily as the geometric and topographic influences on the flow. The following analysis suggests that a reasonable first approximation is to assume it is everywhere small.

In order to test the usefulness of the theoretical analysis leading to equation (8.14), a sequence of calculations was performed with data from the Muddy Creek bend depicted in figure 8.8. In brief, the centreline slope, $\frac{\partial E_o}{\partial s}$ was assumed

constant through the bend, with a value assigned from the field data (.001404). The cross-stream variation in elevation was then calculated as

$$E = E_0 - \frac{\varrho n < u_s >^2}{g(1-N)R} \tag{8.15}$$

The cross-stream variation in boundary shear stress was then computed from equation (8.10). In order to compare these calculated values with observations, the total average boundary shear stress for the bend (55 dynes/cm^2) was related to the bend averaged mean velocity (55 cm/sec) employing a drag coefficient, C_D, i.e.

$$< u_s > = \left[\frac{2\tau_b}{C_D \varrho} \right]^{1/2} \tag{8.16}$$

in which C_D was found to equal 3.61×10^{-2}, and each calculated boundary shear stress was corrected to a vertically averaged downstream velocity.

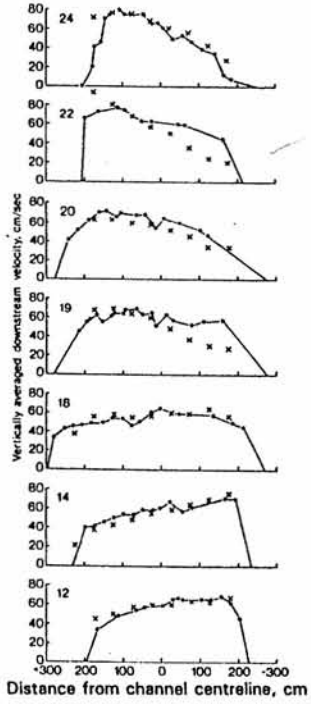

Figure 8.10 Predicted (crosses) and observed vertically averaged downstream velocity in Muddy Creek study bend. Flow section locations are shown in figure 8.8. Flow fields for this stage are graphed in figure 11 of Dietrich and Smith (1983)

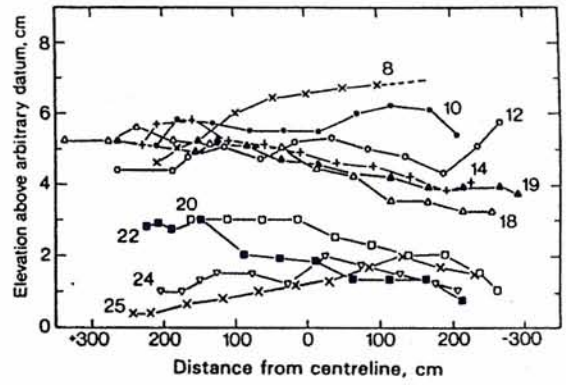

Figure 8.11 Water surface topography for ten cross-sections on Muddy Creek study site. Section locations shown in figure 8.8a. Section 8 is about 5 m upstream of 10 (figure 17 of Dietrich and Smith, 1983). Arbitrary datum. Water surface is tilted upslope in upstream near concave bank area over pool. In axis of bend where channel widens local surface slope is very flat or reversed. Similarity in average cross-channel slope is due to nearly constant radius of curvature from 14 to 20

Despite the approximate nature of the calculated vertically averaged velocity, the comparison between predicted and observed velocity fields in most sections appears to be quite good (figure 8.10). Careful inspection of each section reveals, however, that the cross-stream structure of the predicted velocity disagrees systematically with the observed: at sections 14, 19, 22 the velocity varies too much across the channel, and at sections 12 and 24 it varies too little. Improvements could perhaps be made by repeating the above calculations after adjusting the local centreline slope to satisfy continuity requirements such that the discharge is the same at each cross-section. This may improve predictions at 20 and 24, but such an adjustment was performed and found to be quite small despite the field observation that the centreline slope varies considerably through the bend.

Figure 8.11 shows the successive cross-stream water surface profiles through the meander. From sections 12 to 19 the cross-stream slope is greater than the downstream one, the downstream centreline slope is close to zero and over the upstream part of the pool and middle part of the bar (18–19) the local downstream water surface slope is reversed, an observation not predicted by the above equations and demonstrating the importance of momentum forces which will carry the flow through local reaches with water-slope reversal.

A more critical test of this model involves converting the calculated boundary shear stress to a local boundary shear stress responsible for sediment transport (by removing resistance effects due to the point bar and dunes) in order to

compare predicted and observed bedload transport fields. Dietrich et al. (1984) have shown that channel average ratio of total boundary shear stress to the boundary shear stress available for sediment transport is about 3.7. Division of this ratio into the calculated boundary shear stress and comparison with observed bedload fields (Dietrich and Smith, 1984a figure 17) showed relatively close agreement for section 14, but poor agreement in sections 18 through 24 (figure 8.12). In sections 20 to 24 the bedload transport maximum is near the centre of the channel (but as can be inferred from figure 8.10, the predicted boundary shear stress and bedload transport maximum is close to the outside bank). No comparison could be made at 19B because bedload transport was not measured at this section. The poor agreement between predicted and observed bedload transport fields towards the downstream outside bank arises in part from failure to include the topographically-induced convective acceleration in equations (8.8) and (8.9).

The simple calculations performed above suggest that theories that include forms of equations (8.1) and (8.2) will be fairly successful in predicting flow, but much less successful in predicting boundary shear stress and bedload transport fields in curved channels. In part due to the lack of laboratory or field observations on sediment transport, theories that have been employed to predict

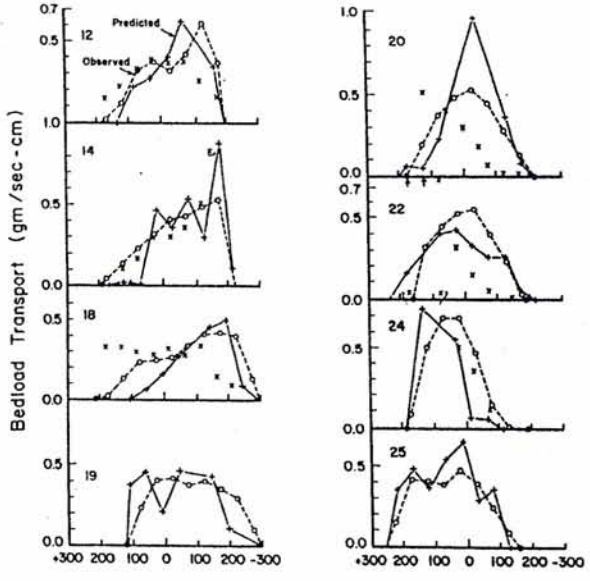

Figure 8.12 Observed bedload transport fields (circles), transport predicted from local velocity measurements (plusses), and that predicted from the simple theory for boundary shear presented in the text. Arrows in section 22 indicate substantial over-prediction of (from left to right) 2.2 and 1.2 gm/cm-sec

bed morphology are rarely tested for their accuracy in predicting sediment transport fields. Nonetheless this simple approach sheds light on the dominant processes controlling bends and may be useful in obtaining quick approximate solutions for practical purposes.

SEDIMENT TRANSPORT PROCESSES IN BENDS

Flow over bar-pool topography and through a sequence of alternate curves generates forces that result in a cross-stream skewed boundary shear-stress field with a distinct zone of maximum boundary shear stress that in the downstream direction shifts back and forth across the channel in response to local channel morphology. In the mobile-bed case, downstream increases or decreases in the local boundary shear stress will either cause erosion or deposition, or at equilibrium, be balanced by corresponding convergent or divergent sediment transport. Transport directions of bedload are controlled by near-bed fluid vectors and cross-channel and downstream bed slope. Transport direction of suspended load will be influenced by flow direction throughout the water column. In strongly heterogeneous grain-size mixtures of sediment, another response to systematic boundary shear-stress change may be a coarsening or fining of the bedload which in turn adjusts the sediment flux rate, as bedload transport rate is strongly grain-size dependent. In partially mobile beds or ones that rarely experience shear stresses significantly above critical, such as is the case in many gravel-bedded streams, response to spatial variations in the boundary shear-stress field may be largely through bed grain-size adjustment. Hence, prediction of channel-bed morphology requires that a quantitative linkage be established between topographically controlled boundary shear-stress fields and the grain-size, bed-slope and flow direction-influenced sediment transport fields. This linkage is currently being explored both theoretically and through field studies.

Forces on a bed particle and channel morphology

Figure 8.13 illustrates the forces acting to move bed particles in a curved channel. Fluid forces are lift and drag, F_L and F_D respectively. When the particle rests or rolls on an inclined bed, the body forces, F_g, have a cross-stream component, F_{gx}, and a component normal to the bed (not shown here). Generally, the downstream component is small when the grain contacts the bed; either at its initial motion, or as it rolls, or when it bounces during saltation, an opposing frictional force is exerted on the grain by the bed. For simplicity, this opposing force is not shown in figure 8.13. The direction in which a particle moves in the cross-stream plane is determined by the magnitude and direction of near-bed

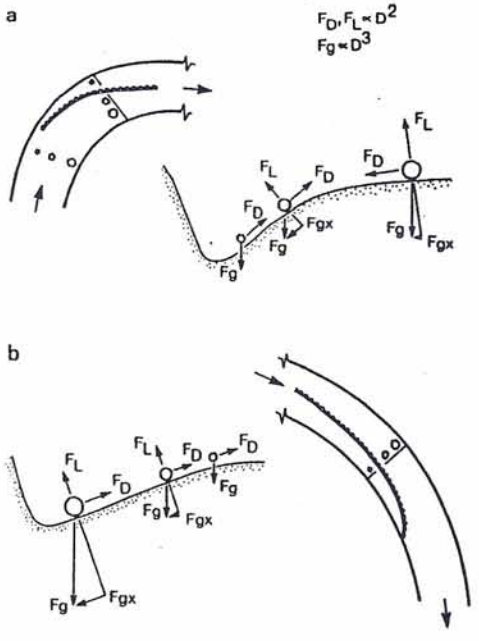

Figure 8.13 Forces acting on particles on or near the bed that contribute to motion. Opposing frictional resistance of the bed not shown. Forces are lift (F_L), drag (F_D), and gravity (F_g) with the cross-stream component of gravity also shown (F_{gx}). Saltating particles once off the bed no longer experience F_{gx} and F_L is negligible. Sorting in bends results from grain size dependent response to fluid and gravitational forces on sediments moving on a cross-stream sloping point-bar surface against an inward component of the curvature-induced secondary circulation. The gravitational acceleration is proportional to the cube of the particle diameter, D, and the fluid forces are proportional to the square of the diameter. The resultant of these forces is further inward for small grains than for large grains. Also, the finest bedload grains will saltate one to three grain diameters off the bed or be intermittently suspended, in which case the particles move primarily in the near-bed flow direction

flow and bed slope. In figure 8.13a the case of shoaling-induced outward flow over the bar top is shown. Typically, at the entrance to the bend in a meander train where shoaling will be most significant, the largest particles in transit are near the inside bank and the smallest ones are near the outside one. All three forces on the particle will tend to give it an outward transport component; in order to move, it must also overcome the frictional resistance of the bed. In contrast, on the bar slope and into the pool, the inward component of drag on resting and rolling particles is opposed by a component of lift, acting perpendicularly to the bed and by the outward component of the particle weight,

F_{gx}. Note that once grains leave the bed they are no longer acted upon by a cross-stream component of particle weight or by a significant fluid lift. Consequently, particles that mostly saltate or are intermittently suspended will tend to travel in the direction of the local fluid motion. Wiberg and Smith (described in Dietrich and Smith, 1984a, pp. 1375–6) have found that flow deflection inward of only a few degrees will compensate for the lateral component of lift on sand on an out-sloping bar.

In figure 8.13b, which represents the downstream end of laboratory flumes with constant curvature, or the zone well downstream of the curvature maximum in natural channels, the same set of forces are shown but the inward component of drag acts over much of the bar (as described in a previous section) and the largest particles are in the pool. The shift in cross-stream grain size distribution from a to b, which could be the downstream end of a, is a consequence of submerged weight and drag-force differences on large and small particles. As Dietrich et al. (1979, p. 313) described, and Parker and Andrews (1985) subsequently modelled, the outward gravitational component is proportional to the cube of the grain diameter, whereas the fluid drag is proportional to the diameter squared. Hence for the same near-bed velocity, large particles will tend to roll outward against the inward flow and smaller ones will be carried inward toward the shallow water. This is the essence of the sorting process in bends. It may also apply to bar units in general in either straight or braided channels.

Many different quantitative formulations of the force balance dictating particle motion have been proposed for both static (e.g. Odgaard, 1981; Ikeda, 1982) and moving particles (e.g. Engelund, 1974; Nelson and Smith, 1985; Parker and Andrews, 1985 (and references therein); Odgaard, 1986). They differ primarily in how lift and bed frictional forces are determined. Linking a particle equation with equation (8.7) to calculate local boundary shear stress and with conservation of mass equations for sediment transport allows prediction of both grain sorting and channel topography. Theories vary greatly as to how this linkage is obtained but have focused on predicting equilibrium bed topography in bends.

The two basic hypotheses for what controls equilibrium morphology in curved channels are:

1 equilibrium is achieved when the cross-stream component of the particle weight (and fluid lift) is exactly balanced by the inward component of the fluid drag due to secondary circulation: particles therefore travel along lines of equal depth (e.g. Allen, 1970; Kikkawa et al., 1976; Bridge, 1977);
2 equilibrium is achieved when the outward shifting zone of maximum boundary shear stress is balanced by convergent sediment transport caused by net outward bedload flux toward the pool (Dietrich and Smith, 1984b; Struiksma et al., 1985).

The difference in these two hypotheses is similar to the distinction between fully developed flow and flow which changes downstream as a consequence of bed topography and planform curvature effects. Unless significant grain-size adjustments can occur in response to shifting boundary shear-stress fields (as suggested by Bridge and Jarvis, 1982), the hypothesis of net outward bedload transport would seem necessary. Once shifting of the boundary shear-stress field through the bend has occurred, and the downstream boundary shear stress remains constant (if this occurs), net cross-stream bedload transport is no longer necessary. During stage change in a channel in which the bed remains mobile, the shoaling hypothesis leads to specific predictions which are supported by field observations (Dietrich and Smith, 1984a). Stage rise will reduce the shoaling effect, but the high boundary shear stress will still shift outward, and without outward flow over the bar, deposition will occur. In the pool, the lack of cross-stream sediment transport will cause erosion. Conversely, during stage decline the bar top and bar slope will be eroded and the pool aggraded. In the following, a brief review is given of quantitative approaches to predicting bed topography in bends.

Bridge (1977) employed the Engelund (1974) theory for flow and boundary shear stress in bends following a sine-generated curved path. He assumed that at equilibrium there is no net cross-stream discharge of sediment, and that instead grain size tracks the boundary shear-stress distribution. Through a bend, as the zone of maximum boundary shear stress shifts outward, the coarsest particles follow it and suppress a tendency for sediment transport to increase. Fine particles move inward to the low shear-stress zone, and the maximum bedload transport zone tends to stay toward the centre of the channel. The Engelund model upon which Bridge's theory is based has several deficiencies (see comments in Dietrich and Smith, 1984a; Parker and Andrews, 1985), both in its basic flow equations and particle force balance. For channels that are approximately sine-generated, Bridge (1984) has shown that his theory stimulates observations reasonably well. As shown above, however, it is fairly simple to get the correct basic average velocity field, which in turn gives the approximate boundary shear stress, and because bedload particle size is proportional to the imposed boundary shear stress, the correct grain size distribution. The bedload transport field is not predicted with this model, and the estimates of bed topography at Muddy Creek (figures 3 and 6 in Bridge, 1984) are fairly crude. Nonetheless, the analytical expression is very simple and it performs impressively well. Dietrich and Smith (1984a, figure 18) show quantitative evidence that the bedload maximum is offset toward the centreline due to grain-size effects in a short section of their bend, but they also demonstrate that this effect in their study site is of secondary importance: net cross-stream transport of most of the bed particles still occurs and the bedload maximum crosses the channel. Bridge and Jarvis (1982) have

proposed that their field data support the assumptions of the model, but this is debatable (see review in Dietrich and Smith, 1983; 1984a). They argue that there is field evidence for a downslope-upslope force balance on individual bed particles (their figure 23). However, they do not use observed cross-stream near-bed flow orientations, but rather compute it from an equation they show to be very approximate. In addition, the proposed cross-stream force balance equation (equation 13 of Bridge and Jarvis, 1982) has a large number of redundant terms which, when eliminated, reduce their force balance to the statement (see their equation 15) that the dimensionless Shields number ($\tau_b/(\varrho_s-\varrho)gD$; ϱ_s is grain density) is about 0.3, which must be within an order of magnitude of the correct value. Hence a logarithmic plot of the cross-stream forces on a particle must yield approximately a good comparison, but such an analysis cannot be used to test the cross-stream force balance hypothesis.

The sorting model of Parker and Andrews (1985) is based on an even simpler representation of the flow processes in a bend. They assume that the boundary shear stress is everywhere the same and that sorting arises purely due to cross-stream bed tipping and the relative action of inward (everywhere) boundary shear stress and outward gravitational acceleration on the particle. Bed topography is calculated from the theory. They obtain an analytical solution which allows estimation of the path of 'coarse' sediment through a succession of bends. One result of their theory is the prediction that channels with high width to depth ratios will have less cross-stream shifting of coarse sediment. Although not tested with field data, nor explained physically, this conclusion may be correct. As discussed above, bends of large width–depth ratio have broad, nearly flat point-bar tops. Both the cross-stream gravitational force and the near-bed inward flow will be weak on this surface. Consequently, sediment will not be quickly segregated by size across the channel.

Bridge (1977; 1984), Parker and Andrews (1985) and many others use the approximation that the angular deviation (δ) of the boundary shear-stress vector from the downstream direction is proportional to the flow depth, h, and inversely proportional to the radius of curvature, r:

$$\tan\delta = C\,h/r \qquad (8.17$$

Dietrich and Smith (1983) showed, however, that the assumptions used to derive equation (8.17) from the equation of motion require that the flow be steady and uniform; hence it is strictly applicable only to fully developed flow in parts of bends. Odgaard (1986) has developed a modification of equation (8.17) that allows inclusion of shoaling effects.

The models of Hasegawa and Yamaoka (1984), Nelson and Smith (1985) (which is built upon the Smith and McLean (1984) flow theory) and Odgaard (198

have included the shoaling effect (figure 8.13a). The flow theory of Hasegawa and Yamaoka appears to predict quite well the vertically averaged velocity vectors in their laboratory meanders. Their particle equation leads to a cross-stream sediment transport equation (their equation (9)) similar to that of Engelund's equation (68) (Engelund, 1974), but they did not report a comparison between observed and predicted bed topography in their channels. Dietrich and Smith (1984a), however, employed Engelund's equation to predict the net cross-stream discharge of bedload through their study bend (figure 8.14). In the co-ordinate system of figure 8.6, the equation can be written as

$$\frac{Q_n}{Q_s} = \left[\nu - \frac{7h}{r} + \frac{1}{tan\phi} \frac{\partial h}{\partial n} \right] \tag{8.18}$$

in which Q_n and Q_s are the downstream and cross-stream sediment transport, ν is the ratio of vertically averaged cross-stream velocity to vertically averaged downstream velocity, 7 is the constant in equation (8.17) and ϕ is the dynamic friction angle. The first term was interpreted to represent the shoaling effect; the second term, the secondary circulation effect; and the third, the cross-stream gravitational effect. Using equation (8.18) very crudely, Dietrich and Smith (1984a) found it gave approximately correct results (figure 8.14).

Odgaard's model differs significantly from that of Nelson and Smith or Hasegawa and Yamaoka in that it includes several empirical approximations that permit an analytical solution. The Nelson and Smith model was not published at the time of writing, but preliminary applications to the field observations in Muddy Creek

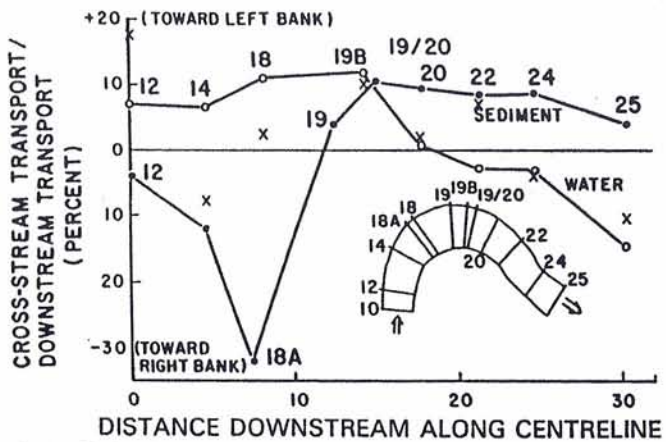

Figure 8.14 Ratio of cross-stream to downstream transport of bedload and water as a function of distance downstream from section 12. Predicted ratio for bedload from Engelund (1974) equation also shown as crosses. Geometric crossing to downstream bend is below 22. Negative values are toward right, which in the upstream bend is the inner bank.

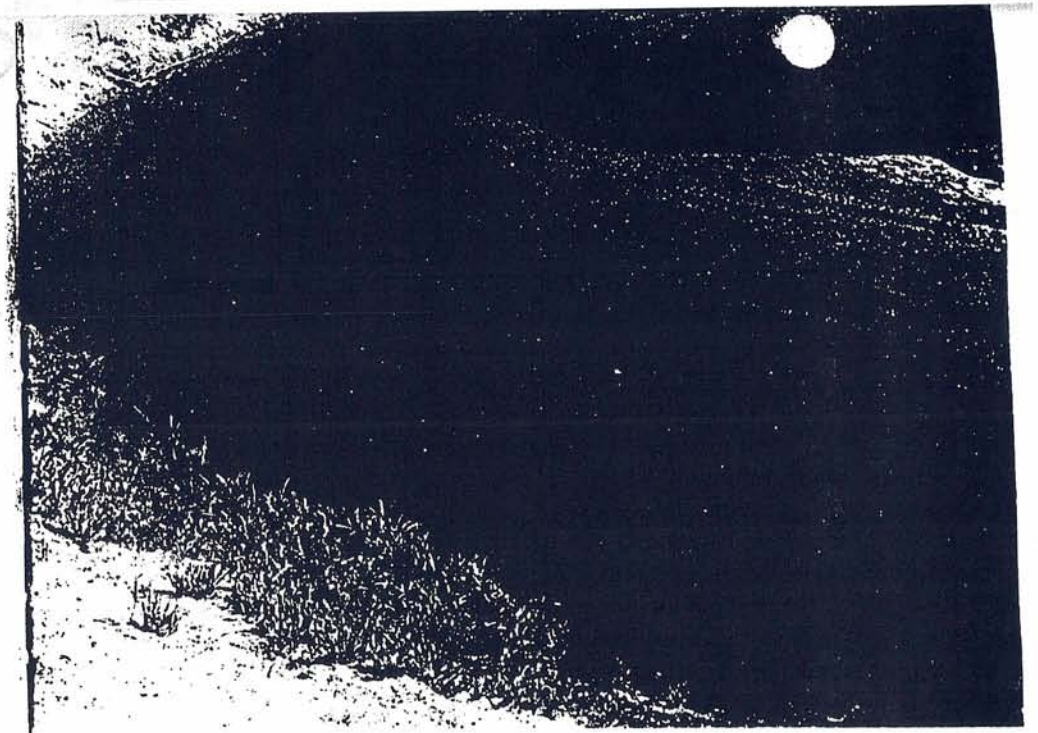

Figure 8.15 Well developed oblique dunes with spurs in a sharp bend in Muddy Creek, Wyoming. Spurs migrated inward along trough. Obliquity due to skewed boundary shear stress field with maximum near inside bank

(data of Dietrich and Smith, 1983; 1984a), appear to be very promising. However, there are very few other data with which to test a thorough, physically based model for flow and channel morphology, a point discussed further below

There is one other effect not illustrated in figure 8.13 that may be important in controlling the sorting and morphology in sand-bedded rivers. Figure 8.15 shows a sharp bend upstream from the Muddy Creek study site. At least eight sinuous, oblique dune crests are clearly visible stretching from the point-bar top to the deep pool. Parallel ridges run between dune crests (called 'spurs' by H. Ikeda, personal communication, 1985), and in the deeper water towards the left bank, relatively deep local scour holes have formed. Any oblique step to a mean flow direction will generate a downstream current along the step (figure 8.16). Because crest migration speed is proportional to boundary shear stress in bends, the cross-stream variation in boundary shear stress should produce strong skewing of the dune crests, so that their downstream ends are near the convex bank in the upstream part of the bend (figure 8.17) and shift towards the concave bank in the downstream part (Dietrich et al., 1979; Dietrich and Smith, 1984a). In the upstream part of the bend the troughs of dunes provide low-velocity zones that allow the cross-stream pressure gradient force to overcome

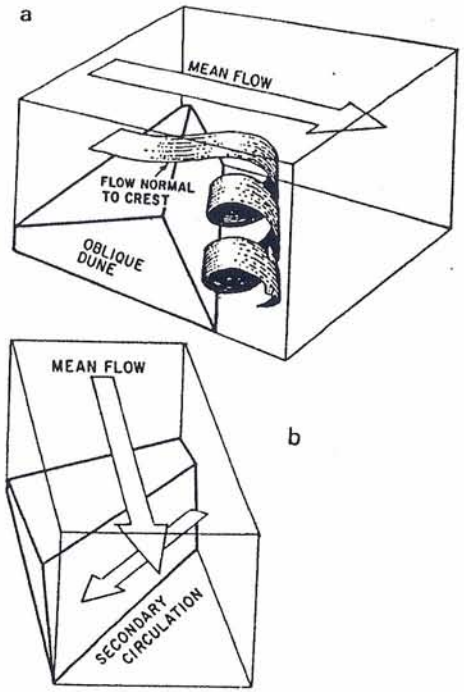

Figure 8.16 Deflection of flow near crest, formation of separation cell and generation of cross-stream current due to bedform obliquity to the near flow (a). Direction of mean flow and secondary circulation (and near-bed troughwise current) induced by bedform obliquity in the trough (b).
Illustration by Leslie Reid

the shoaling-induced outward flow that would otherwise occur, and the obliquity of the dunes adds an additional cross-stream pressure gradient that results in strong troughwise current towards the convex, inside bank. The spurs here and in other bends were observed migrating upslope towards the inside bank. During net deposition the combined migration of the dunes and spurs will generate trough cross-stratification. In the upstream part of the bend the troughwise current may be strong enough to prevent net cross-stream rolling of the coarsest particles toward the pool and to cause net inward transport of sediment even though near-bed flow near the crests is directed outwards due to shoaling effects. This hypothesis was proposed by Dietrich and Smith (1984a) to explain the observed net cross-stream sediment transport near the crossings where the cross-stream bed slope is negligible (sections 12 and 24) and further into the bend (sections 14, 18A) in a direction opposite to that expected from shoaling effects

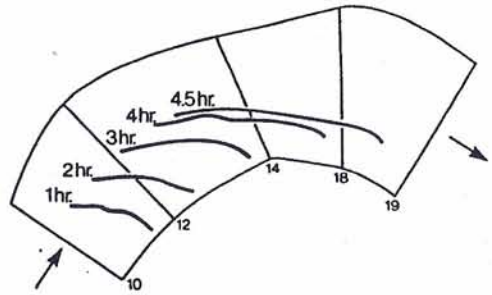

Figure 8.17 Predicted dune crest migration through the Muddy Creek study bend. Lines represent crest location at various hours after entering the reach at section 10 with crest parallel to section line. Prediction used a map of observed downstream dune-crest velocities to compute displacement distance of the crestline increments after one hour and, for the last calculation, one half-hour. Progressive skewing of crest line results from cross-stream decreasing boundary shear stress from inside bank to the outer and corresponding declining crest speed. Note the nearly uniform crest speed along the inside bank. Prediction was not carried further because dunes did not propagate across channel; instead new dunes formed in deeper water and grew with the addition of sediment rolling down the point-bar slope to become the predominant bedforms in the downstream part of the bend.

(figure 8.14). They documented strong troughwise transport along oblique dunes in these sections (Dietrich and Smith, 1984a, figure 21; Dietrich, 1982, figure 5-32). They also noted that where the dunes were nearly perpendicular to the flow, low-velocity zones were created in which large particles could roll across the channel into the deeper water. Where the downstream boundary shear-stress maximum had crossed into the pool downstream of the apex of the bend, the dunes rotated and generated troughwise currents capable of transporting sediment towards the pool in a region where the average near-bed flow orientation is inward.

These observations suggest that dunes, by their effect on local boundary shear-stress directions, may modify the pattern of sorting and equilibrium bed morphology otherwise dictated by shoaling effects, curvature secondary circulation, and differential movement due to relative grain size dependent response to gravity and drag. Near-bed influence of dunes on flow is probably ubiquitous in sand-bedded river bends. In order to appreciate this effect more fully, a summary of Muddy Creek observations follows, with illustrations that complement those presented by Dietrich and Smith (1984a). I will first comment on problems of sediment transport measurement.

Mapping sediment transport fields in river bends

Unlike flow-field observations, where during steady flow fairly sparse data fields and short sampling periods may still give roughly correct results, under-sampling

of sediment transport fields, particularly when the bed is not clearly visible, is probably worse than no sampling at all. Poor data may appear to give support to incorrect hypotheses, or more typically are used to suit one's hypotheses. Sediment flux rates, both in suspension and as bedload, are highly variable in space and time, even when on average the local flux may be nearly constant. In sand-bedded streams, bedload and suspended load vary greatly due to bedform migration and periodic suspension of particles associated with unsteady wakes of major bedforms (see below and figure 8.19). In order to map the bedload transport field, repeated sampling is essential at carefully selected locations (if the bed is clearly visible), or at numerous locations across the channel. A single or few measurements at many positions across the channel cannot (except by chance) accurately portray the transport fields (see comments in Dietrich and Smith, 1984a). This is true both for bedload and suspended load. Bedload sampling methods required to map transport vectors are discussed by Dietrich and Smith.

No data on the bedload transport fields of gravel-bedded rivers are, to the author's knowledge, published. This deficiency will be overcome, but it will also require repeated sampling at several positions across the channel. Researchers working on gravel bedload transport have found it highly variable (e.g. Hubble et al., 1985) due, at least in part, to pulses of sediment, or bedload sheets (Whiting et al., 1985), that can dominate transport rates at low excess boundary shear stress. In this case as well as the dune-covered sand-bed case, transport measurements should be repeated enough to average over at least one wavelength of the migrating bed feature causing bedload fluctuations. In any sediment transport study, mass conservation equations of the flow (if data are available), as defined by equation (8.5), or of the sediment transport (equation 4 of Dietrich and Smith, 1984a) must be employed to define correctly the downstream and

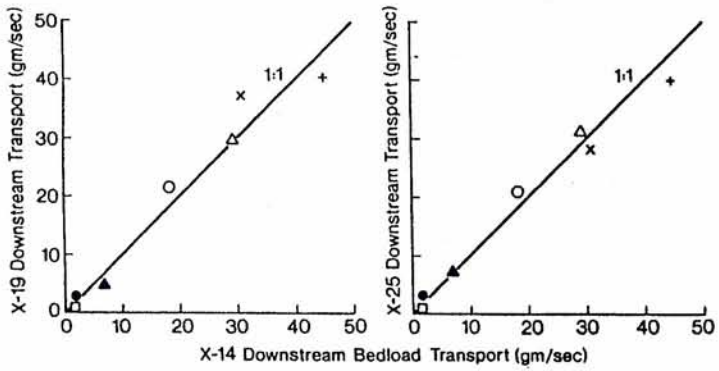

Figure 8.18 Comparison of measured downstream bedload transport rate for 7 sizes of sediment at three sections in bend (see figure 8.21 for explanation of symbols)

cross-stream components of sediment transport. Furthermore, because ultimately the paths which individual grains take through the bend are of great importance, it is useful to compare transport rates for individual size classes at successive sections. Figure 8.18 shows such a comparison for three sections in the Muddy Creek bend.

Bedforms and sediment transport processes in a sand-bedded meander

Figure 8.19 (a–f) shows a downstream sequence of photographs of the Muddy Creek stream bed taken with a camera suspended about 7 m over the channel during the same period as the bedload and flow measurement. Flow is towards the bottom of the figure. Specific locations and scales are given in the figure caption. The photographs are representative of the dune geometry, because for a given reach of the bend, the dunes tend to have a roughly constant orientation, amplitude and crest speed. The dunes are strongly three dimensional across the channel, with sinuous, often oblique crests. In the deep water in the upstream part of the bend where the sediment is fine sand, ripples predominate, but ripples and ripple-like low crested bedforms also occur throughout the bed. Ripples are superimposed on upstream strongly oblique limbs (figure 8.19a) in the lee of the upstream point bar. Three crest lines of these limbs are clearly visible. Sequential photographs (which were taken at ten minute intervals for several hours at each location through the bend) showed that as the dunes propagated into the bend, their outer limbs slowly merged onto the new stagnant outermost limb visible in the photograph.

Further downstream, the limb is abandoned, the dunes skew under the cross-stream gradient of boundary shear stress (highest near the inside bank), and develop spurs which tend to migrate inward (figure 8.19b–d). Two dune fields start to develop in this reach (b to d) on either side of the centreline, approximately where the shoaling effect of near-bed outward flow ends and inward secondary flow is strong (figure 8.8). Near-bed velocity on the stoss side of the dune in figure 8.19 is convergent toward the centreline in this reach. Average dune crest height was greatest (6 to 17 cm) close to the centreline throughout the bend. In many places, but particularly in association with the highest-crested dunes, the separation cell in the trough of dunes would break, rotate and generate a boil-like structure, sometimes capable of suspending even the coarsest sand on the bed. Distinct local clouds of suspended sediment can be seen in the centre of figures 8.19b and d. Because of favourable sun angle, the distorted water surface due to a boil is clearly visible in two places in figure 8.19b.

The break-up of the bed into two dune fields ends between section 19 and 20 (figures 8.19e and 8.20a, b) where the shoaling-induced outward flow terminates and the boundary shear stress and bedload transport maxima have

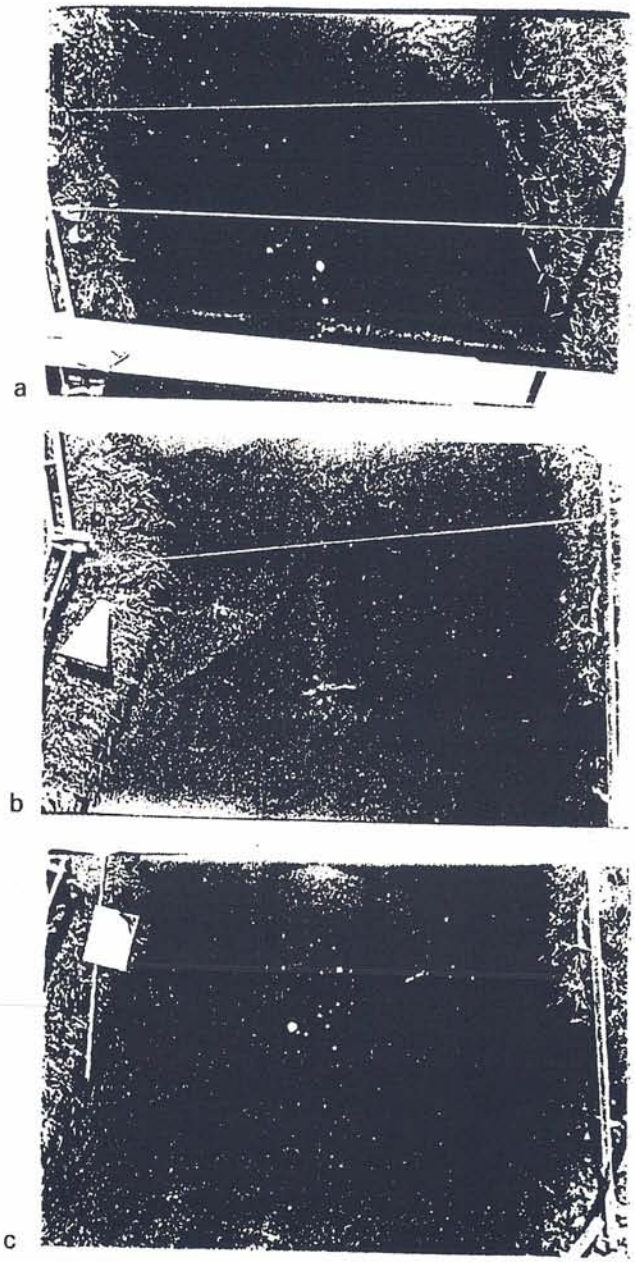

Figure 8.19 Photographs of streambed taken from camera suspended approximately 7 m above the bed. Scale differs somewhat in each picture. (a) bed between cross-sections 10 and

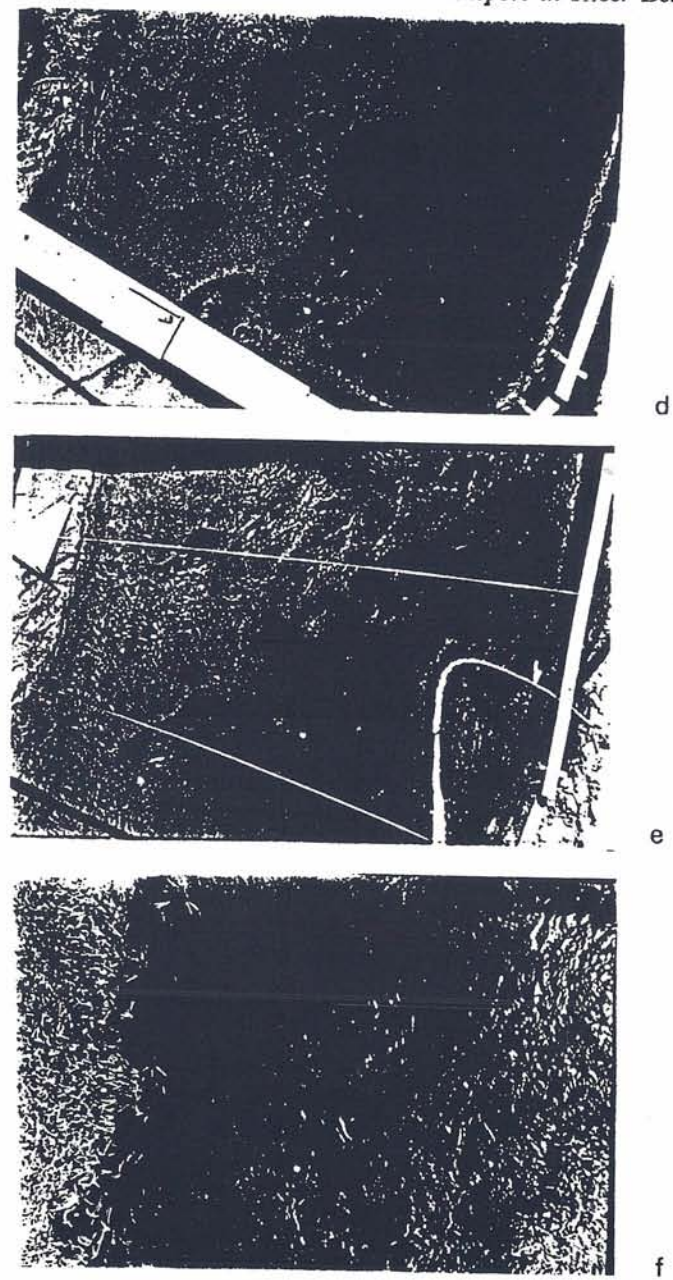

12; (b) tape is stretched across section 14; (c) bed between sections 14 and 18; (d) bed betwee sections 18 and 19; (e) bed between sections 19 and 20; (f) bed upstream of section 2

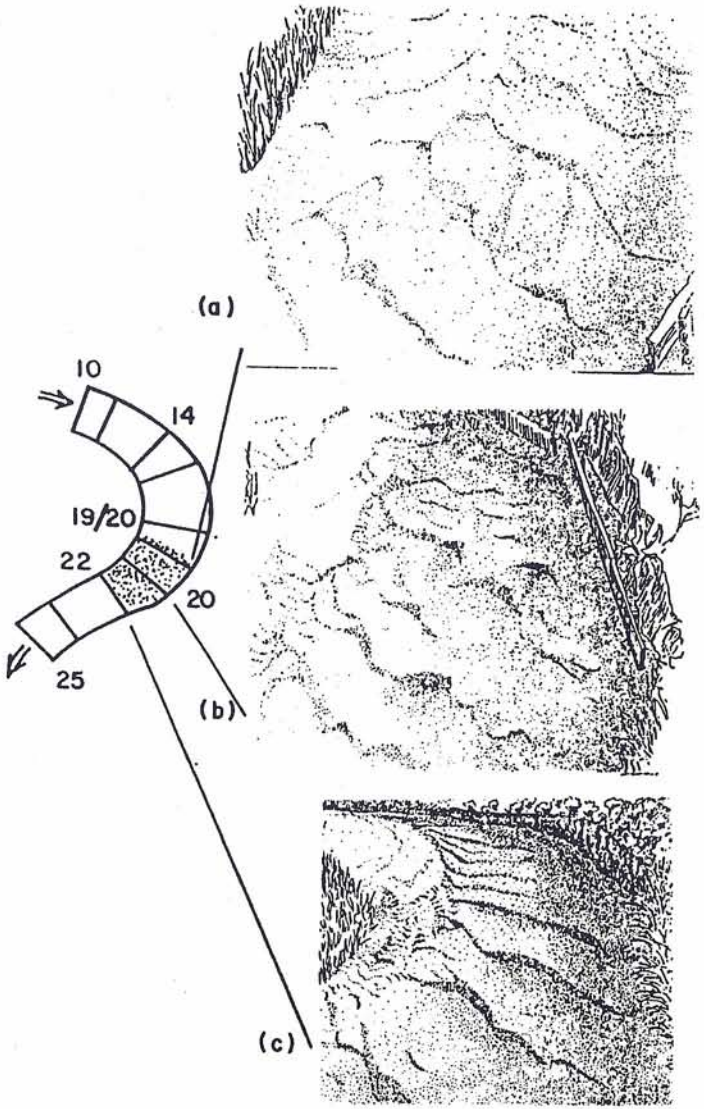

Figure 8.20 Sketches of stream channel and bed looking from outer bank upstream. The map gives locations of viewer. The channel bed at section 19/20, corresponding to E in figure 8.19, is shown in (a). In (b) the left bank at section 20 is at the downstream end of the closest railing. Section 19/20 is near the intersection of the two railings. In (c) the railing has been deleted to simplify the drawing. The sketch is from the left bank at section 22. Note that in all three drawings greatest dune height is at the transition from the shallow point-bar surface to the steep side-slope of the point bar near the channel centreline, not in the deepest water. This is also where significant local suspension of sediment occurred due to boils. Sketches are by Lenora Wilson (from Dietrich and Smith, 1984a)

shifted towards the pool. In figure 8.19e, three almost evenly spaced, large-amplitude dunes are visible on the point-bar slope and two spurs extend downstream from the middle crest. Further downstream towards section 24 (figure 8.19f and 8.20c), sun reflection off the turbulent eddies shed from the bank obscure the well developed dunes developed in the deeper water. As seen in figure 8.19a, ripple-covered limbs of major dunes swing into the shallow flow, merge and stagnate.

The suspended-sediment transport field appears to be strongly controlled by the ejection of bed material by boil-like features from the large-crested dunes near the centre of the channel. The maximum suspended sediment load (two to three times cross-sectional average) stayed slightly towards the outside of the centreline (see Dietrich and Smith, 1984a) throughout the meander. On the other hand, median settling velocity of the vertically averaged suspended-sediment load varied across the channel in proportion to the local boundary shear stress, and the cross-stream variation of the median settling velocity paralleled that of the bedload, although the values were much lower. Strong suspension of bed material should tend to counteract the inward secondary current effects, preferentially carrying smaller particles higher in the flow toward the pool and larger ones near the bed towards the inside bank. In Muddy Creek, this effect is small because of the small loads involved. In streams with high concentrations this may be an important process in sorting sediment and adjusting the bed topography. Regrettably there appear to be no other detailed field data with which to examine this hypothesis, although Ikeda (1985) has made an important theoretical investigation of this problem.

In order to describe briefly the cross-stream transport and sorting of sediment in the bend, figures 8.21 and 8.22 are included to show the observed downstream bedload transport rates for seven settling-velocity classes of sediment, and the cross-stream structure of the median grain size through the bend. Figure 8.14 shows that in the bend depicted in figure 8.19, net inward transport occurred in the upstream region (from photographs a to c), a reach where the channel width increases from about 4.6 to 6.0 m. Relative to the channel centreline, the width to the base of the outside bank stayed essentially constant; most of the increase of the width of active sediment transport was along the inner bank. Hence, net inward cross-stream transport developed. The dunes appear to have contributed significantly to generating inward transport. As Dietrich and Smith (1984a) described, the large-crested dunes and corresponding deep scour hole near the channel centreline (figure 8.19b) allowed inward cross-channel flow near the bed to develop completely to the down-stream crest. Also the dune obliquity generated strong inward troughwise transport.

Through this reach (sections 12–18A, figure 8.21 and 8.22) the downstream transport fields for different sediment sizes varied little. The maximum flux

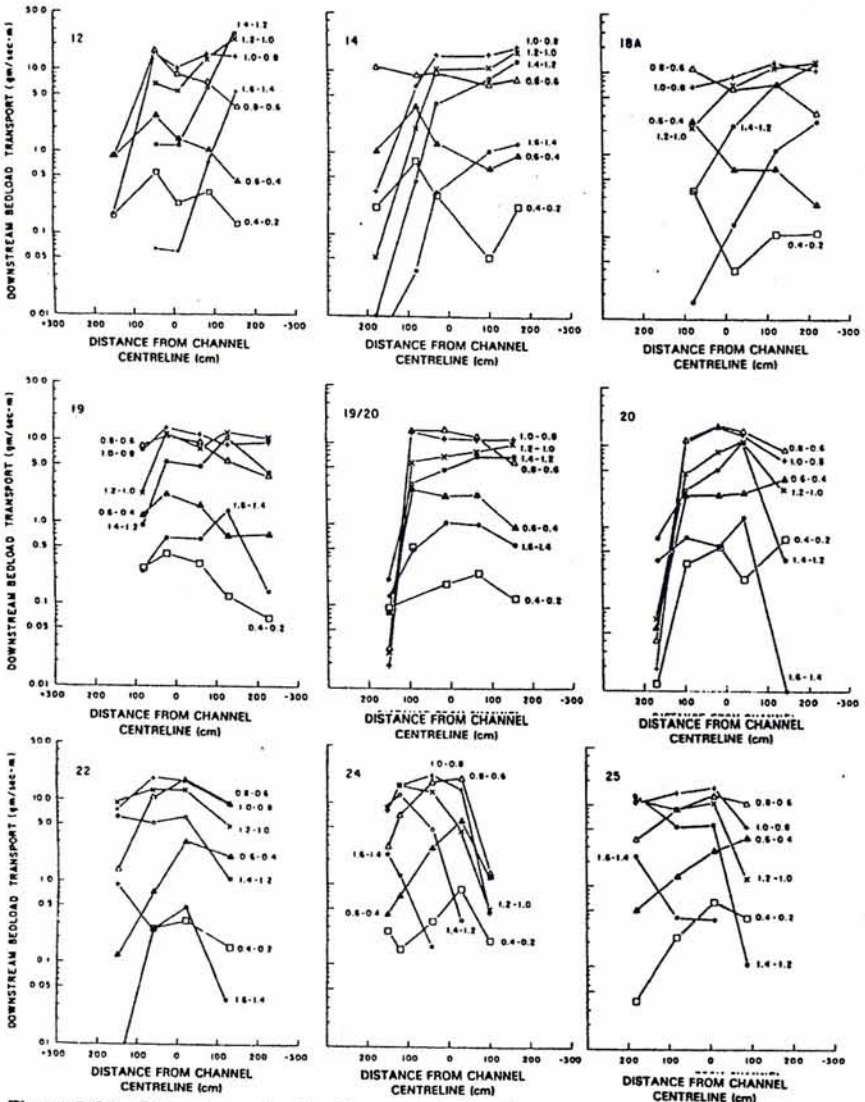

Figure 8.21 Downstream bedload transport fields of seven size classes of settling velocity at nine sections through bend. Vertical axis is bedload transport in gm/sec-100 cm. Symbols used correspond to logarithmic settling-velocity intervals and represent the same interval at each section. Conversion from settling velocity to grain size is given in figure 8.22. Values shown in that graph, 0.2 and 1.6, correspond to 0.12 mm and 8.6 mm, respectively. Note that the logarithmic vertical scale, used in order to show transport in all size classes, reduces the cross-stream slope of the transport fields.

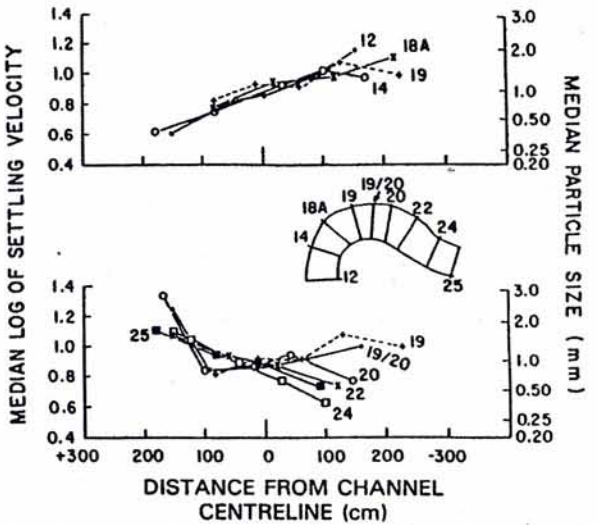

Figure 8.22 Variation of median $\log_{10}$ settling velocity and particle size across the channel at successive sections. The map shows the section locations (from Dietrich and Smith, 1984a)

rate for particles coarser than about 0.7 mm was near the inside bank, for particles finer than about 0.5 mm the flux rate was systematically greater toward the outer bank. Note that the bulk median grain size for Muddy Creek is 0.7 mm (or 0.94 logarithmic settling velocity). In this reach most of the sediment would follow a zig-zag path; outward or weakly inward over the stoss side of the dune and strongly inward along the trough.

From sections 18 through 24, the zone of maximum boundary shear stress shifted outwards and net cross-stream transport of sediment towards the pool was about 10 per cent of the downstream sediment flux rate (figure 8.14). This small cross-stream component shifted the centre of mass of the bedload transport field from 75 cm towards the inner bank to 75 cm towards the outer bank – that is, through about 150 cm or close to 40 per cent of the channel width occupied by a mobile bed. Although the median particle size (or settling velocity) quickly increases near the pool (figure 8.22) the position of the maximum flux rate for each size (or settling velocity) class shifts progressively outwards, only moving close to the outer bank at the exit of the bend. Hence, figure 8.21 and 8.22 do not show the same patterns, and shifting median grain size through the bend does not accurately portray the outward shift of bedload sediment.

The effect of dunes on the cross-stream transport and sorting is extensively discussed elsewhere (Dietrich and Smith, 1984a). The principal findings are illustrated in figure 8.23. The shoaling-induced outward flow near the bed is

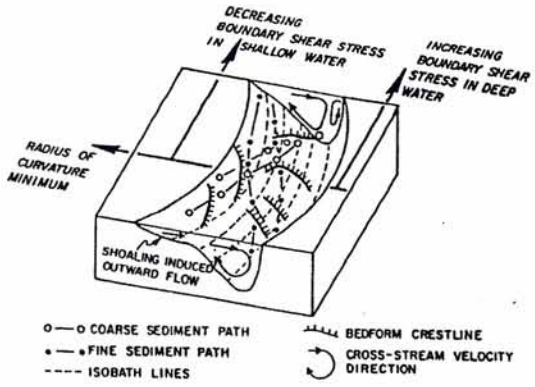

Figure 8.23 Processes controlling bed morphology and particle sorting in a river meander. Flow is from lower to upper end of figure
(from Dietrich and Smith, 1984b)

effective on the shallow point-bar surface (figure 19d and e, figure 8.20a and b) in causing net transport of the bulk of the sediment to the edge of the point-bar top at the break in slope. In the troughs of the thin, oblique dunes on the bar top, weak troughwise currents can carry just the fine sediment brought up the point-bar slope by the inward near-bed flow there. The troughs, then, create a low velocity region on the gently sloping point-bar surface where large and small particles can cross paths (figure 8.23). On the bar slope the large particles will tend to roll outward against the inward near-bed flow and finer particles will tend to roll less far or be carried inwards. Rolling is enhanced in the troughs oriented normal to the flow direction (figure 8.19e). On dunes that extend across the bar slope, grain avalanching during dune migration will also produce an outward transport component. Further downstream in the bend strong dune obliquity generates a troughwise current in a direction opposite to the near-bed flow on the stoss side of dunes which is capable of transporting large amounts of sediment across the channel. Although clearly influencing local sediment flux rate and direction, the net effects of dunes on sorting, sediment transport processes and channel morphology are not easily defined. In the upstream part of the bend, oblique dunes prevent particles from rolling into the pool, and as Dietrich et al. (1979) proposed this may cause the upstream end of the pool to deepen and reduce the local boundary shear stress to critical. An opposite effect may occur in the downstream end of the bend where rolling in dune troughs and troughwise transport towards the pool may reduce the cross-stream slope needed to generate sufficient outward transport to match the outward shifting boundary shear-stress maximum. Overall, the effects of dunes on sorting may be to increase the strength of the cross-stream variation in sediment size. These effects will only be identified

once theory has advanced to the point of being sufficiently physically-based so that failure to include dune influences can be shown to give an inaccurate result.

CONCLUSION: PROBLEMS REMAINING

Although considerable progress has been made in recent years in understanding the mechanics of flow and sediment transport in bends, many questions remain. Most of these questions derive from an almost complete lack of detailed field measurements. Channel-bed morphology appears to be strongly influenced by the width–depth ratio; with increasing width relative to depth, the point-bar surface flattens and extends well across the channel. No detailed measurements of the kind needed to investigate mechanics and test theory have been collected in bends of high width–depth ratio. Many large amplitude bends tend to become non-symmetric and develop multiple bars within a single major bend. There are very few field data on flow and sediment transport processes in such bends; consequently the mechanisms responsible for planform deformation and multiple bar formation are not well understood. The role of intermittent suspension of bed material in the sorting and bar development of fine sand-bedded streams is virtually unexplored in the field. Similarly, detailed field investigations of flow and sediment-transport processes in gravel-bedded river bends have not been reported. Here grain-size adjustments may play a major role in accommodating shifting boundary shear-stress fields.

Until thorough data on sediment transport and boundary shear-stress fields are generated during geomorphologically significant stages, theoretical investigations cannot be properly tested. Theories are becoming progressively more physically based and are employing fewer imposed, mathematically convenient assumptions. This makes such investigations complex and dependent on computer-based numerical analysis. In parallel with these advances, engineers are improving their analytical solutions using a blend of empiricism and theory such that fairly accurate predictions can be made of flow, boundary shear-stress fields and bed topography.

This chapter has focused on processes in a bend of a given planform. As in this case, theoretical investigations of meander evolution are more advanced than the available field data. There remains the fundamental problem of making definitive field measurements that link the fluid mechanics of the flow through a bend with the erosion rate and sediment transport processes on and at the base of the bank.

ACKNOWLEDGEMENTS

The field data from Muddy Creek were collected in collaboration with J. Dungan Smith, Thomas Dunne and several of their graduate students. Support was in part provided

through National Science Foundation grant ENG78-16977 and CEE-8307142. Ron Shreve provided valuable comments on a draft of the chapter. Discussions with J. Nelson, J. Dungan Smith and Peter Whiting were particularly helpful. Eileen Hughes assisted in the final preparation of the manuscript.

REFERENCES

Allen, J. R. L. 1970: *Physical Processes in Sedimentation*. London: Allen and Unwin.

Brice, J. C. 1984: Planform properties of meandering rivers. In C. M. Elliott (ed.), *River Meandering: Proceedings of the Conference Rivers '83*, Am. Soc. Civ. Eng., 1-14.

Bridge, J. S. 1977: Flow, bed topography, grain size and sedimentary structure in bends: a three dimensional model. *Earth Surface Processes*, 2, 401-16.

Bridge, J. S. 1984: Flow and sedimentary processes in river bends: comparisons of field observations and theory. In C. M. Elliott (ed.), *River Meandering: Proceedings of the Conference Rivers '83*, Am. Soc. Civ. Eng., 857-72.

Bridge, J. S. and Jarvis, J. 1976: Flow and sedimentary processes in the meandering river South Esk, Glen Cova, Scotland. *Earth Surface Processes*, 1, 303-36.

Bridge, J. S. and Jarvis, J. 1982: The dynamics of a river bend: a study in flow and sedimentary processes. *Sedimentology*, 29, 499-541.

Chitale, S. R. 1970: River channel patterns. *J. Hydraulic Div., Am. Soc. Civ. Eng.*, 96, 201-21.

Church, M. and Jones, D. 1982: Channel bars in gravel-bed rivers. In R. D. Hey, J. C. Bathurst and C. R. Thorne (eds), *Gravel-bed Rivers* Chichester: Wiley, 291-338.

DeVriend, H. J. and Geldof, H. J. 1983: Main flow velocity in alternating river bends. *J. Hydraulic Engineering, Am. Soc. Civ. Eng.*, 109, 991-1011.

Dietrich, W. E. 1982: Flow, boundary shear stress and sediment transport in a river meander. Unpublished PhD dissertation, Seattle: University of Washington.

Dietrich, W. E. and Smith, J. Dungan, 1983: Influence of the point bar on flow through curved channels. *Water Resources Research*, 19, 1173-92.

Dietrich, W. E. and Smith, J. Dungan, 1984a: Bedload transport in a river meander. *Water Resources Research*, 20, 1355-80.

Dietrich, W. E. and Smith, J. Dungan, 1984b: Processes controlling the equilibrium bed morphology in river meanders. In C. M. Elliott (ed.) *River Meandering: Proceedings of the Conference Rivers '83*, Am. Soc. Civ. Eng., 759-69.

Dietrich, W. E., Smith, J. Dungan and Dunne T. 1979: Flow and sediment transport in a sand-bedded meander. *J. Geol.*, 87, 305-15.

Dietrich, W. E., Smith, J. Dungan and Dunne, T. 1984: Boundary shear stress, sediment transport and bed morphology in a sand-bedded river meander during high and low flow. In C. M. Elliott (ed.), *River Meandering: Proceedings of the Conference Rivers '83*, Am. Soc. Civ. Eng., 632-9.

Elliott, C. M. (ed.) 1984: *River Meandering: Proceedings of the Conference Rivers '83*, Am. Soc. Civ. Eng.

Engelund, F. 1974: Flow and bed topography in channel bends. *J. Hydraulic Div., Am. Soc. Civ. Eng.*, 100, 1631-48.

Ferguson, R. I. and Werritty, A. 1983: Bar development and channel changes in the gravelly River Feshie, Scotland. *Spec. Pub. Int. Ass. Sediment*, 6, 181-93.

Forbes, D. L. 1983: Morphology and sedimentology of a sinuous gravel-bed channel system: lower Babbage River, Yukon coastal plain. *Spec. Publs. Int. Ass. Sediment*, 6, 195-206.

Friedkin, J. F. 1945: *A Laboratory Study of the Meandering of Alluvial Rivers*. Vicksburg, Mississippi: US Waterways Experimental Station.

Fujita, Y. 1982: On the formation of stream channel pattern. In *Proceeding of Third Congress of the Asian and Pacific Regional Division of the International Association for Hydraulic Research*, 276-87.

Hasegawa, K. 1983: *A study on flows and bed topographies and planforms of alluvial meanders*. Unpublished PhD dissertation, Hokkaido University.

Hasegawa, K. and Yamaoka, I. 1984: Phase shifts of pools and their depths in meander bends. In C. M. Elliott (ed.), *River Meandering: Proceedings of the Conference Rivers '83*, Am. Soc. Civ. Eng., 885-94.

Hey, R. D. and Thorne, C. R. 1975: Secondary flows in river channels. *Area*, 7 191-5.

Hooke, J. M. 1984: Changes in river meanders: a review of techniques and results of analyses. *Progress in Physical Geography*, 8, 473-508.

Hooke, J. M. and Harvey, A. M. 1983: Meander changes in relation to bend morphology and secondary flows. In J. D. Collison and J. Lewin (eds), *Modern and Ancient Fluvial Systems*. Oxford: Basil Blackwell, 121-32.

Hooke, R. L. 1974: Distribution of sediment transport and shear stress in a meander bend. *Uppsala Univ. Naturgeografiska Inst. Rapport*, 30.

Hooke, R. L. 1975: Distribution of sediment transport and shear stress in a meander bend. *J. Geol.*, 83, 543-65.

Hubble, D. W., Stevens, H. H., Skinner, J. V. and Beverage, J. P. 1985: New approach to calibrating bedload samples. *J. Hydraulic Engineering, Am. Soc. Civ. Eng.*, 111 677-94.

Ikeda, S. 1982: Incipient motion of sand particles on side slopes. *J. Hydraulic Engineering*, 108, 95-114.

Ikeda, S. 1984: Flow and bed topography in channels with alternate bars. In C. M Elliott (ed.), *River Meandering: Proceedings of the Conference Rivers '83*, Am. Soc Civ. Eng., 733-46.

Ikeda, S. 1985: Bed topography in bends of sand-silt rivers. *J. Hydraulic Engineering Am. Soc. Civ. Eng.*, 111, 1397-411.

Jackson, R. G. 1976: Depositional model of point bars in the Lower Wabash River *Journ. Sed. Pet*, 46, 579-94.

Kalkwijk, J. P. Th. and DeVriend, H. J. 1980: Computations of the flow in shallow river bends. *J. Hydraulic Research*, 18, 327-42.

Keller, E. A. 1972: Development of alluvial stream channels: a five-stage model. *Geol Society of America Bulletin*, 83, 1531-40.

Keller, E. A. and Melhorn W. 1973: Bedforms and fluvial processes in alluvial stream channels: selected observations. In M. Morisawa (ed.), *Fluvial Geomorphology*, SUNY Binghamton: Publication in Geomorphology, 253-83.